



저작자표시-비영리-변경금지 2.0 대한민국

이용자는 아래의 조건을 따르는 경우에 한하여 자유롭게

- 이 저작물을 복제, 배포, 전송, 전시, 공연 및 방송할 수 있습니다.

다음과 같은 조건을 따라야 합니다:



저작자표시. 귀하는 원저작자를 표시하여야 합니다.



비영리. 귀하는 이 저작물을 영리 목적으로 이용할 수 없습니다.



변경금지. 귀하는 이 저작물을 개작, 변형 또는 가공할 수 없습니다.

- 귀하는, 이 저작물의 재이용이나 배포의 경우, 이 저작물에 적용된 이용허락조건을 명확하게 나타내어야 합니다.
- 저작권자로부터 별도의 허가를 받으면 이러한 조건들은 적용되지 않습니다.

저작권법에 따른 이용자의 권리는 위의 내용에 의하여 영향을 받지 않습니다.

이것은 [이용허락규약\(Legal Code\)](#)을 이해하기 쉽게 요약한 것입니다.

[Disclaimer](#)

공학석사 학위논문

**Thermal-Structural Analysis of Micro
Reactor Core Using Coupled OpenFOAM and
Heat Pipe Code**

**OpenFOAM-히트파이프 연계 코드를 이용한
초소형 원자로 노심 열-구조 해석**

2021년 2월

서울대학교 대학원
에너지시스템공학부
정 명 진

**Thermal-Structural Analysis of Micro Reactor Core
Using Coupled OpenFOAM and Heat Pipe Code**

**OpenFOAM-히트파이프 연계 코드를 이용한 초소형
원자로 노심 열-구조 해석**

지도교수 조 형 규

이 논문을 공학석사 학위논문으로 제출함

2021년 2월

서울대학교 대학원
에너지시스템공학부
정 명 진

정명진의 석사학위 논문을 인준함

2021년 2월

위 원 장

김응수

부위원장

조형규

위 원

박병하



Abstract

Thermal-Structural Analysis of Micro Reactor Core Using Coupled OpenFOAM and Heat Pipe Code

Myungjin Jeong

Department of Nuclear Engineering

The Graduate School

Seoul National University

Recently, various types of micro reactor concepts have been proposed and relevant researches, developments, and demonstrations are in progress. Among them, heat pipe cooled reactor is considered to be a strong candidate with several advantages. The heat pipe cooled reactor has the core which consists of multiple fuel rods and heat pipes, installed in a solid structure called a monolith. It has the advantages of compact design, easy installation portability, and improved system reliability and stability. The development of the heat pipe cooled reactor is led by LANL, Westinghouse, and OKLO.

There are several issues in the core design of the heat pipe cooled reactor. It is necessary to integrate a number of fuel rods and heat pipes in a small volume for the land-based heat pipe cooled reactor with MWe scale power. This integration increases the temperature gradient within the core structure that induces high thermal stresses. In addition, high temperature and power fluctuation due to frequent load following make solid core volume expand, and reactivity feedback

occurs as the neutron leakage changes. In addition to it, there are safety criteria for heat pipe cooled reactor operation conditions, which vary depending on the reactor characteristics, hence a high fidelity multi-physics simulation is needed.

For the multi-physics simulation, the coupling between heat pipe thermal analysis code and reactor core thermal-structural analysis code is required. For this, INL, KAERI, etc. conducted researches on the core analysis of heat pipe cooled reactors, and SNU-ANL also performed coupled analysis for the heat pipe cooled reactor core.

The purpose of this study is an improvement of reliability in the design and safety analysis of a heat pipe cooled micro reactor by developing a high fidelity multi-physics simulation tool. For this, an open source-based CFD code OpenFOAM, was used, which has a basic stress and expansion analysis solver required for multi-physics analysis.

To analyze the thermal stress of the heat pipe cooled reactor core, OpenFOAM solid mechanics solver was improved. The existing “solidDisplacementFoam” solver in OpenFOAM has been modified so that it became possible to handle multiple materials and their varying properties according to temperature. In addition, a feature that reads external volumetric heat field was implemented for coupling with neutronics code, and an external data exchange boundary condition for coupling in a solid surface was added.

A coupling system between OpenFOAM and a heat pipe code ANLHTP was established. OpenFOAM and ANLHTP were externally coupled through Python code. OpenFOAM provides heat transfer rate and ANLHTP calculates interface temperature. To compensate for the limit of ANLHTP and reflect the axial temperature distribution, the location at which the variables are exchanged was set

as the wick-vapor interface. For the convergence of the boundary temperature, Picard iteration was used with the fixed point method and secant method.

In order to confirm the appropriateness of the coupling, steady-state and transient thermal-structural analyses of the heat pipe cooled reactor core were performed using the coupled code. The unit cell(7HP) problem was analyzed, and the temperature distribution of the monolith and fuel rods, and the thermal stress distribution in the monolith were confirmed. The temperature and thermal stress were compared with the MegaPower reactor core analysis performed by INL, and the OpenFOAM-ANLHTP coupled code was qualitatively assessed.

As a demonstration of the coupled code system, analysis for the Minicore conceptual problem, which was designed by ANL, was conducted. The core incorporates 84 fuel rods and 55 heat pipes and has 132 kW power. From the steady-state and transient analyses, the thermal-structural analysis capability of the coupled code was successfully demonstrated. Furthermore, the results presented that the specified geometry, power, and cooling conditions may exceed the ASME maximum allowable stress limit. Thus, modification of geometry or thermal condition is desired in the future and the coupled code could be used effectively for this purpose.

.....
Keywords: Multiphysics analysis, Micro reactor, Reactor core analysis, Thermal-structural analysis, Stress analysis, OpenFOAM, Heat pipe,

Student Number: 2019-20171

List of Contents

Abstract	i
List of Contents	iv
List of Tables	vi
List of Figures	vi
Chapter 1. Introduction	1
1.1 Background.....	1
1.1.1 Heat pipe cooled micro reactor.....	1
1.1.2 Open source-based CFD software OpenFOAM.....	11
1.2 Objective and Scope	13
Chapter 2. Customization of OpenFOAM Solid Mechanics Solver	15
2.1 Solid Mechanics Solver	15
2.1.1 solidDisplacementFoam	15
2.1.2 Verification of the thermal-structural analysis solver	17
2.2 Solver Customization	30
2.2.1 Modification of the solver	30
2.2.2 Boundary condition for external coupling.....	33
Chapter 3. Establishment of Code Coupling System	34
3.1 ANLHTP	34
3.2 Coupling Strategy	38
3.2.1 Supervising python code	40
3.2.2 Interface temperature convergence strategy	42
Chapter 4. Demonstration of the Coupled OpenFOAM-ANLHTP Code	45
4.1 Unit Cell (7HP) Problem	45
4.1.1 Problem specifications and modeling.....	45
4.1.2 Calculation results	51
4.1.3 Comparison with reference data	58
4.2 Minicore Problem	60
4.2.1 Problem specifications and modeling.....	60

4.2.2	Calculation results	62
4.2.3	Parametric study for design improvement.....	74
Chapter 5. Conclusions.....		81
5.1	Summary.....	81
5.2	Recommendations	83
References.....		84
국문초록.....		88
감사의 글.....		91

List of Tables

Table 1.1 Stress analysis results of the MegaPower reactor (Sterbentz et al., 2017)	6
Table 1.2 Reactivity feedback coefficients of INL design A (Hu et al., 2019)	6
Table 1.3 Reactivity feedback coefficients of Aurora (OKLO, 2020)	6
Table 2.1 Properties of heated beam problem	19
Table 2.2 Heated beam problem case 1 calculation results	19
Table 2.3 Heated beam problem case 2 calculation results	19
Table 2.4 Properties of steady-state cylinder problem	23
Table 2.5 Calculation results for steady-state cylinder problem	23
Table 2.6 Properties of transient cylinder problem	27
Table 2.7 Calculation results of transient cylinder problem	27
Table 2.8 Modification of OpenFOAM solid mechanics solver	32
Table 4.1 Geometric information of unit cell problem	48
Table 4.2 Material properties of the heat pipe cooled reactor core	48
Table 4.3 Information of the sodium heat pipe	48
Table 4.4 The heat pipe heat sink temperature of the Minicore problem	76

List of Figures

Figure 1.1 Conceptual figure of the heat pipe cooled reactor	7
Figure 1.2 The ASME code Maximum allowable stress for SS316	8
Figure 1.3 Transient fuel temperature following the loss of heat sink (Hu et al., 2019)	8
Figure 1.4 Sockeye-Bison-Rattlesnake-MAMMOTH coupled analysis result (Martineau, 2019)	9
Figure 1.5 Preliminary core design of heat pipe cooled reactor for space (Choi, 2019)	9

Figure 1.6 ANLHTP-PROTEUS-FLUENT coupled analysis result (Lee, 2019)..	10
Figure 1.7 Simulation of a GODIVA prompt critical burst (Aufiero, 2015).....	12
Figure 1.8 Multi-physics simulation results of a SFR core (Fiorina, 2015)	12
Figure 2.1 Conceptual figure of the heated beam problem	20
Figure 2.2 Displacement and strain result for case 1 of the heated beam problem.....	20
Figure 2.3 Axial stress result for case 2 of the heated beam problem	21
Figure 2.4 Conceptual figure of the steady-state cylinder problem	23
Figure 2.5 Temperature distribution result of the steady-state cylinder problem..	24
Figure 2.6 Inner surface stress result of the steady-state cylinder problem.....	24
Figure 2.7 Outer surface stress result of the steady-state cylinder problem.....	25
Figure 2.8 Conceptual figure of the transient cylinder problem.....	27
Figure 2.9 Inner-outer surface temperature difference of the transient cylinder problem	28
Figure 2.10 Inner surface stress result of the transient cylinder problem.....	28
Figure 2.11 Outer surface stress result of the transient cylinder problem	29
Figure 2.12 The geometry of UO ₂ single rod problem	32
Figure 2.13 The calculation result of UO ₂ single rod problem	32
Figure 3.1 Thermal resistance network of ANLHTP (Lee, 2019)	36
Figure 3.2 Scematic of coupling between OpenFOAM and ANLHTP	36
Figure 3.3 ANLHTP validation results (Lee, 2019).....	37
Figure 3.4 Scematic of data exchange at wick-vapor interface	39
Figure 3.5 Flow chart of coupling procedures in OpenFOAM-ANLHTP	41
Figure 3.6 Boundary temperature convergence during transient calculation	44
Figure 4.1 Schematic of the unit cell	49
Figure 4.2 3D view of unit cell calculation mesh	49
Figure 4.3 Calculation mesh of the heat pipe wick in OpenFOAM	50
Figure 4.4 Thermal analysis result of unit cell in the steady-state calculation.....	53
Figure 4.5 Boundary temperature of HPs in the steady-state calculation.....	53
Figure 4.6 Displacement result of unit cell in the steady-state calculation	54

Figure 4.7 Calculation mesh of unit cell for stress analysis	54
Figure 4.8 Stress analysis result of unit cell in steady-state calculation.....	55
Figure 4.9 Volume expansion of unit cell in steady-state calculation (expanded volume was distorted for visibility)	56
Figure 4.10 Thermal analysis result of unit cell in transient calculation	56
Figure 4.11 Boundary temperature of HPs in transient calculation.....	57
Figure 4.12 Monolith temperature and stress analysis results of unit cell in transient calculation	57
Figure 4.13 Thermal-structural analysis results of the MegaPower reactor core (Sterbentz et al., 2017).....	59
Figure 4.14 Monolith temperature and stress analysis results of unit cell in transient calculation	59
Figure 4.15 Schematic of the Minicore	61
Figure 4.16 3D view of Minicore mesh.....	61
Figure 4.17 Minicore temperature calculation result in steady-state calculation ..	65
Figure 4.18 Heat removal rate of HPs in steady-state calculation.....	66
Figure 4.19 Boundary temperature of HPs in steady-state calculation.....	66
Figure 4.20 The stress analysis result of Minicore for constant temperature boundary case	67
Figure 4.21 The stress analysis result of Minicore for OpenFOAM-ANLHTP coupling case.....	68
Figure 4.22 Volume expansion of unit cell in steady-state calculation (expanded volume was distorted for visibility)	69
Figure 4.23 The peripheral heat pipe failure scenario	69
Figure 4.24 Temperature calculation results of the peripheral heat pipe failure scenario	70
Figure 4.25 Wick-vapor interface temperature of the peripheral heat pipe failure scenario	70
Figure 4.26 Stress calculation results of the peripheral heat pipe failure scenario	71

Figure 4.27 The central heat pipe failure scenario.....	71
Figure 4.28 Temperature calculation results of the central heat pipe failure scenario	72
Figure 4.29 Wick-vapor interface temperature of the central heat pipe failure scenario	72
Figure 4.30 Stress calculation results of the central heat pipe failure scenario	73
Figure 4.31 Heat pipe classification of the Minicore problem	76
Figure 4.32 Heat pipe classification of the Minicore problem	77
Figure 4.33 Temperature calculation results of the Minicore with the heat pipe sink temperature distribution case 1	77
Figure 4.34 Temperature calculation results of the Minicore with the heat pipe sink temperature distribution case 2	78
Figure 4.35 Temperature calculation results of the Minicore with the heat pipe sink temperature distribution case 3	78
Figure 4.36 Temperature distributions of the monolith for different heat sink temperature	79
Figure 4.37 Stress analysis results for different heat sink temperature	80

Chapter 1. Introduction

1.1 Background

1.1.1 Heat pipe cooled micro reactor

Micro reactors are suitable for distributed power systems that require transportability, enhanced safety, and efficient load-following performance. As one of the micro reactor concepts, a liquid metal heat pipe cooled reactor which removes heat from the reactor core using a liquid metal heat pipe has been developing.

A heat pipe is designed for efficient heat removal under high heat flux conditions and is applied to various heat exchange systems such as CPUs and small electronic devices: mobile phones, air conditioning systems, and biofields. The heat pipe cooled reactor has a concept of cooling the small nuclear reactor core which generates MWe-scale power, using several heat pipes driven passively. There is a core in the form of multiple fuel rods and heat pipes installed in a solid structure called a monolith. Then, the heat is transferred from the fuel rod to the power conversion system through the heat pipe installed in the core. Since each heat pipe is physically independent and contains only a small amount of liquid, the risk of loss of coolant is excluded even in the heat pipe broken accident. This heat pipe cooled reactor has emerged as a promising candidate among various micro reactor concepts after the success of LANL's Kilopower reactor experiments in

2018. (Gibson et al., 2018)

As shown in figure 1.1, the development of a heat pipe cooled reactor is being led by LANL, Westinghouse, and OKLO in the United States.

LANL's MegaPower reactor core uses about 20% enrichment UO₂ fuel, and the core is designed to minimize its diameter and reduce weight by utilizing fast neutrons. The heat pipe uses an alkali metal as the working fluid in consideration of the operating temperatures of 650~1000°C. Total 1224 heat pipes are used for 5 MWth power, and each pipe is designed to remove heat up to 5.6 kW. The heat pipes transfer heat from the core to the power conversion system through the heat pipe, and electricity is produced using the air Brayton cycle.

Westinghouse's eVinci reactor can be operated without refuel for 10 years, and passive cooling is possible due to the use of heat pipes. Development of the eVinci is in progress based on MegaPower technology to apply to military bases and remote areas, including automatic operation and load-following capabilities. The eVinci reactor aims to generate electricity of 200 kWe to 5 MWe with operating temperature of 600°C or higher. According to the target milestone proposed in 2019, it is aimed at design completion and demonstration in 2022, testing in 2023, and commercial operation in 2025.

OKLO's Aurora reactor targets 1.5 MWe of electricity and uses a supercritical CO₂ power conversion system. It is operated underground and uses metallic uranium-zirconium alloy fuel (U-10Zr). FSAR(Final Safety Analysis Report) is submitted and evaluation in progress.

Heat pipe cooled reactor core design issue

There are several issues related to the design of the heat pipe cooled reactor core. Fuel rods and heat pipes need to be integrated for MW power of land-based heat pipe cooled reactors. This integration increases the temperature gradient in the structure, induces high thermal stress, and reduces structural integrity. Consequently, the thermal stress issue is included in the safety criteria for the operation of a heat pipe cooled reactor. According to the ASME code, the temperature of the MegaPower reactor's SS316 monolith should not exceed 825 °C, and the stress should not exceed 29.6 MPa based on a temperature of 700 °C. Especially, as shown in figure 1.2, the maximum allowable stress of SS316 decreases rapidly as temperature increases. Because OKLO's Aurora reactor uses metal alloy fuel, there is only fuel temperature criterion: the maximum fuel rod temperature should not exceed 720 °C.

In previous research, INL conducted a PIRT analysis of the MegaPower reactor (Sterbentz et al., 2017). PIRT is an abbreviation of Phenomena Identification and Ranking Tables, which is a structured process to help identify safety-relevant and safety-significant phenomena and assess the importance of such phenomena to the design. The PIRT analyses for the 4 topics were conducted: reactor accident and normal operation conditions, heat pipes, materials, and power conversion.

The most significant findings from the four PIRTs is the phenomena ranked with “high” importance and a corresponding “low” or “medium” knowledge level. These phenomena will impede the deployment of a first-of-a-kind (FOAK) reactor system because either additional research and development or significant system

redesign will be required.

In the reactor accidents and normal operations part, there is stainless steel monolith web failure between HP-fuel channel issue with high importance and low knowledge level. This web failure issue is caused by the high stress at 1mm thick web between fuel and fuel, or between fuel and HP. The high stress may generate defects or cracks at the web region, and a fission product may be transported to HP through failed web region. Therefore, it is necessary to find the potential weak location by calculating the temperature and the corresponding thermal stress in the web region in the monolith.

The thermal-structural analysis of the MegaPower reactor was also performed with PIRT analysis. As a result, as shown in Table 1.1, even during normal operation, the peak stress was 37.1 MPa, exceeding the ASME code limit of 29.6 MPa by about 25%. Since the ASME code limit is usually set as 1/3 of the tensile strength (Maurice Stewart, in Gas-Liquid And Liquid-Liquid Separators, 2008), material failures such as crack do not occur immediately. However, the ASME code specifications and limits should be adequate for long-term operation.

It has been argued that the ASME code limits might not apply to the steel monolith if the monolith is not designated to be a pressure vessel boundary. The final decision would be made by the U.S. Nuclear Regulatory Agency (NRC). For now, the thermal stress issue needs to be further evaluated. (Sterbentz et al., 2018)

In addition, the expansion of volume of the solid core which induced by power fluctuations with high temperature and frequent load following causes neutron leakage change and reactivity feedback. ANL and OKLO performed reactivity feedback coefficient analysis for INL design A and Aurora reactors, respectively. As a result of the analysis, as shown in Tables 1.2 and 1.3, the reactivity feedback

due to thermal expansion was very large.

In order to analyze the thermal stress and reactivity feedback of the heat pipe cooled reactor, the temperature distribution in the heat pipe cooled reactor core and the corresponding thermal expansion must be calculated accurately. INL conducted a multi-physics analysis using the Sockeye-Bison-Rattlesnake-MAMMOTH coupled code to evaluate reactivity feedback in steady and transient conditions. (Martineau, 2019). KAERI conducted a preliminary analysis of a heat pipe cooled reactor for space (Choi, 2019) and a transient heat pipe analysis for a space reactor (Tak, 2020). In addition, KAERI is developing heat pipe analysis code LUPHIS. SNU conducted the coupled heat transfer analysis study in cooperation with ANL using ANLHTTP-PROTEUS-FLUENT coupled code. (Lee, 2019)

Table 1.1 Stress analysis results of the MegaPower reactor (Sterbentz et al., 2017)

Peak von Mises stress [MPa]	
Normal operation	37.1
1 failed HP	154.6
2 failed HP	153.7
3 failed HP	320.4

Table 1.2 Reactivity feedback coefficients of INL design A (Hu et al., 2019)

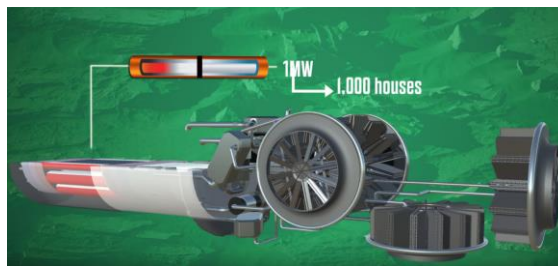
Reactivity feedback coefficients [pcm/K]	
Doppler effect	-0.32
Axial expansion	-0.905
Radial expansion	-1.349
Combined effect	-2.540

Table 1.3 Reactivity feedback coefficients of Aurora (OKLO, 2020)

Reactivity feedback coefficients [pcm/K]	
Fuel thermal expansion	-0.50
Fuel doppler	-0.15
Reactor cell thermal expansion	--0.07
Baseplate thermal expansion	-1.40
Net effect	-2.12



(a) eVinci (Westinghouse, 2020)



(b) MegaPower (LANL, 2019)



(c) Aurora (OKLO, 2020)

Figure 1.1 Conceptual figure of the heat pipe cooled reactor.

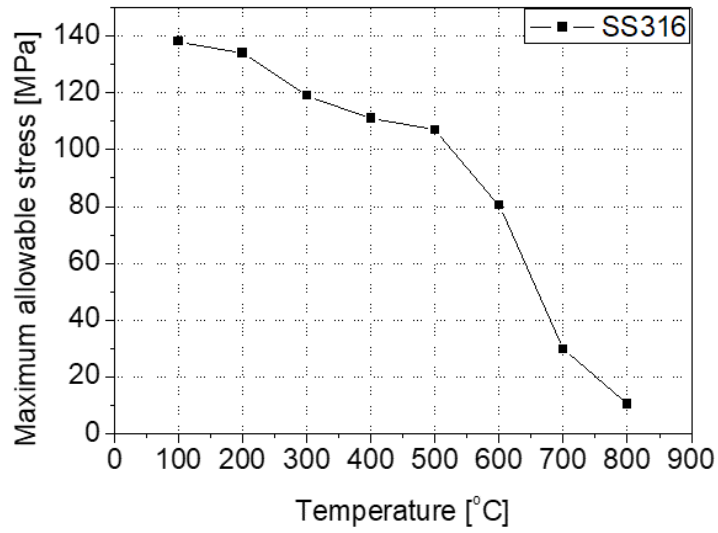


Figure 1.2 The ASME code Maximum allowable stress for SS316

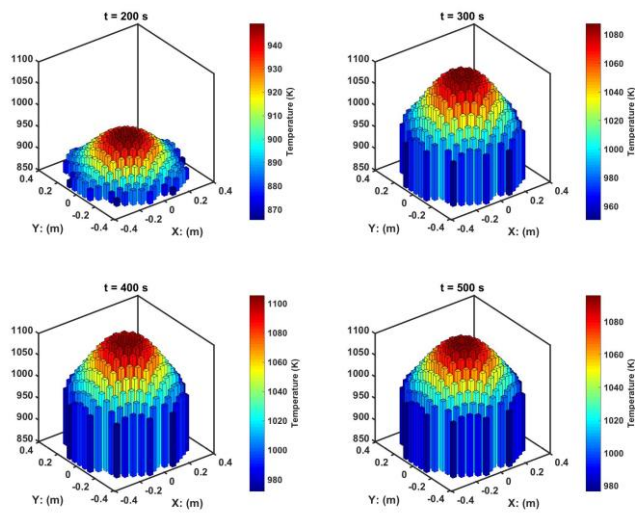


Figure 1.3 Transient fuel temperature following the loss of heat sink (Hu et al., 2019)

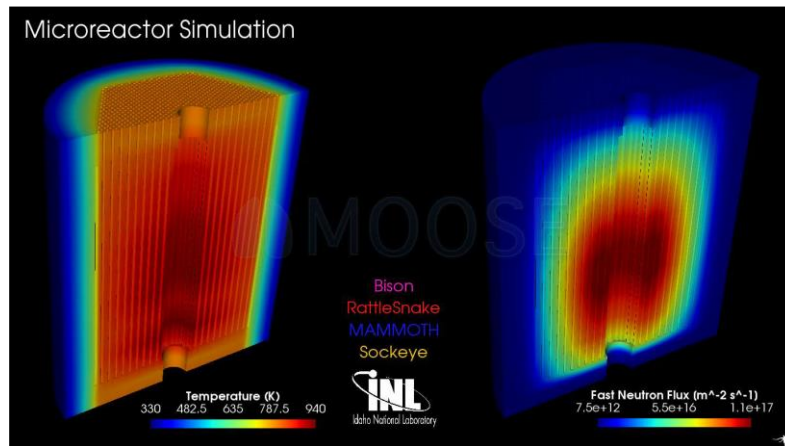


Figure 1.4 Sockeye-Bison-Rattlesnake-MAMMOTH coupled analysis result
(Martineau, 2019)

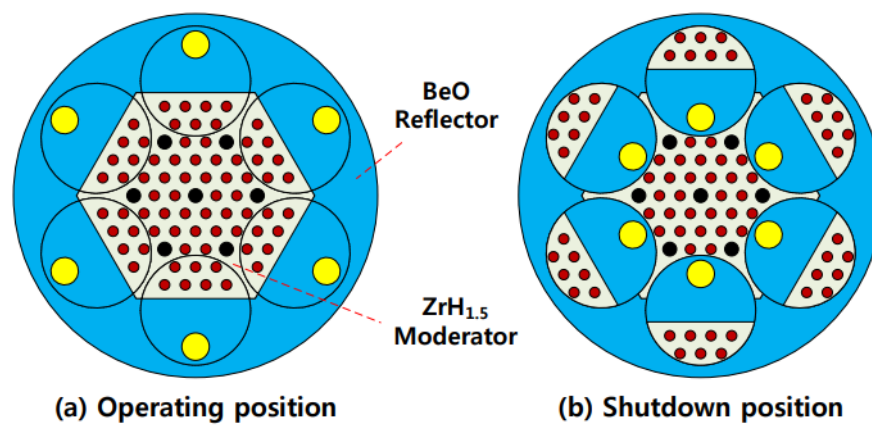


Figure 1.5 Preliminary core design of heat pipe cooled reactor for space (Choi, 2019)

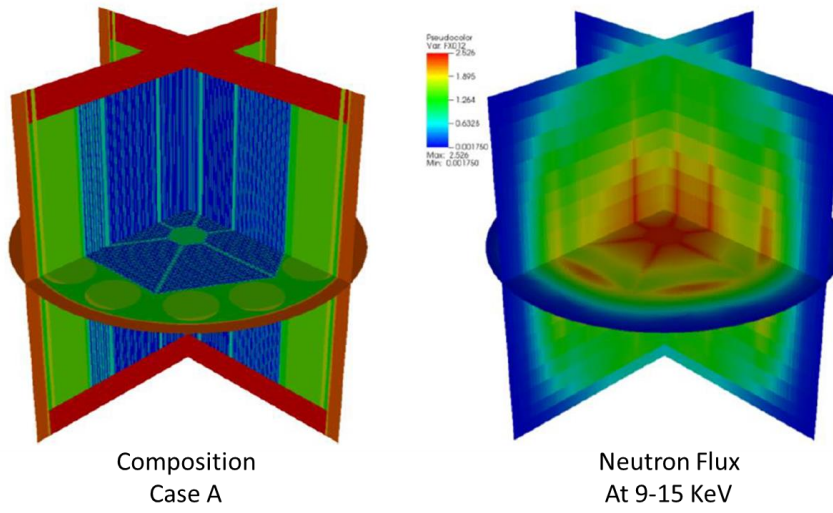


Figure 1.6 ANLHTP-PROTEUS-FLUENT coupled analysis result (Lee, 2019)

1.1.2 Open source-based CFD software OpenFOAM

For the accurate thermal and structural analysis of the heat pipe cooled reactor core, an open source-based simulation tool OpenFOAM was used because it provides stress and expansion analysis solver needed for multi-physics simulation

OpenFOAM (Open source Field Operation And Manipulation) is an open-source computational fluid analysis toolkit based on the GNU General Public License (GPL). It was developed in C++ language and uses the FVM method. The official version of OpenFOAM provides a thermal and structural analysis solver called “solidDisplacementFoam”. OpenFOAM can be used for free, and since it is a code with many users in academia and research circles, it has the advantage of easy modification of the solver.

Thermal-structural analysis using OpenFOAM was also conducted in a nuclear power research group, and in this process, the authors also modified the solver to analyze for their own purpose. In the previous study, the OpenFOAM was coupled with a Serpent Monte Carlo code and a Godiva super-prompt-critical burst has been tested (Aufiero, 2015), and the GeN-Foam multi-physics solver, which is based on the OpenFOAM, was developed and verification for SFR was conducted (Fiorina, 2015).

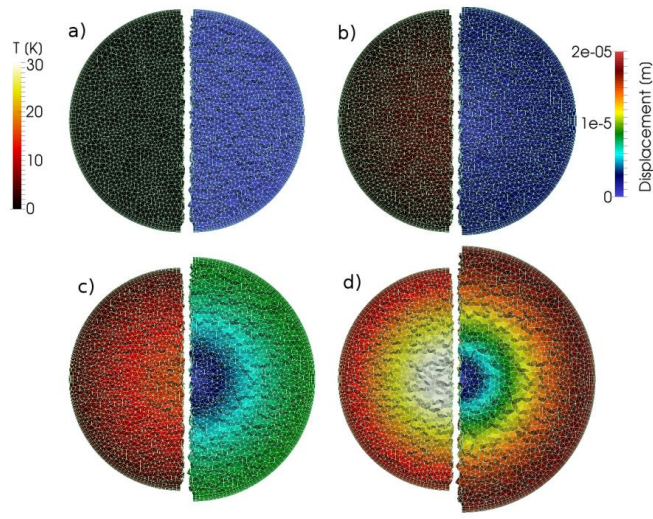


Figure 1.7 Simulation of a GODIVA prompt critical burst (Aufiero, 2015)

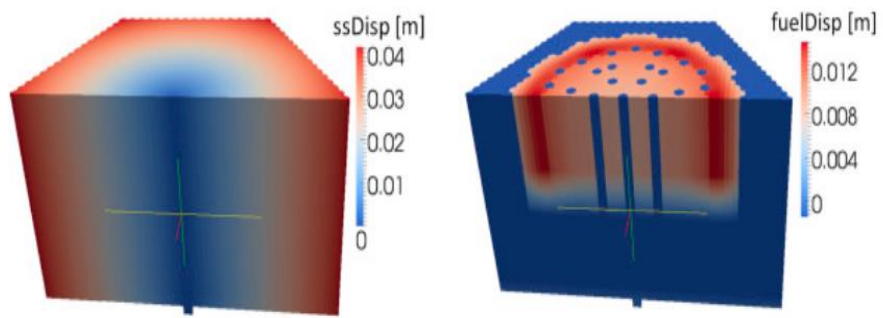


Figure 1.8 Multi-physics simulation results of a SFR core (Fiorina, 2015)

1.2 Objective and Scope

For the design of a heat pipe cooled reactor, it is of great importance to verify if the acceptance criterion of thermal-stress is satisfied and the allowable temperature limits are not violated. It is required that accurate multi-physics can be simulated using validated codes on thermal-structural analysis, heat pipe performance, and neutronic analysis.

The purpose of this study is to improve reliability in the design and safety analysis of heat pipe cooled micro reactor by developing high fidelity multi-physics simulation tool. In this context, the scope of this study can be divided into three parts: the modification of OpenFOAM solver for realistic thermal-structural analysis, the establishment of code coupling, and the demonstration of the coupled code system. The coupled code system was established using OpenFOAM and a heat pipe performance analysis code, ANLHTP, to reproduce the thermo-mechanical behaviors of a heat pipe cooled reactor. Afterward, the demonstration was progressed by comparing the simulation results with reference researches.

At first, the OpenFOAM solver was improved. The solid mechanics solver provided by OpenFOAM which could handle single material is expanded for multiple materials. The material properties treated as a constant in the original solver were converted to a function of temperature. In addition, the modification includes the import of volumetric heat source in each cell considering future coupling work with a neutronics code to reflect reactivity feedback due to thermal expansion. The composition and volumetric heat information for each cell can be read by the solver, which could be provided by an external code. Furthermore, boundary conditions for external data exchange on the solid surface, which is not

included in the original solver, were added for coupling with the heat pipe code.

Secondly, the coupling between OpenFOAM and ANLHTP was conducted. OpenFOAM and ANLHTP were coupled externally using a supervising Python code. OpenFOAM provides the heat transfer rate in the wick-vapor interface, and ANLHTP sends the wall temperature. At this time, during the outer iteration of OpenFOAM, the wall temperature calculated from ANLHTP converged within time step through the Picard iteration

Finally, to demonstrate the performance of the coupled code, a thermal-structural analysis for a heat pipe cooled reactor core was performed. Two cases were analyzed; one is the unit cell(7HP) problem and the other is the Minicore problem. Both the steady-state and a transient condition were analyzed. From the results of the coupled calculations, the temperature distribution of the monolith and the fuel rod, and the thermal stress distribution in the monolith were presented.

In Chapter 2, the procedure of the OpenFOAM solver modifications presented. The modified parts of the thermal-structure analysis solver are described and added boundary condition for external coupling at the solid surface is explained. After that, details of heat pipe code ANLHTP, coupling methodology, and supervising Python code are provided in Chapter 3. The coupling between two codes and the iteration method for the solution convergence is presented. Chapter 4 includes the thermal-structural analysis results for a heat pipe cooled reactor core using OpenFOAM-ANLHTP coupled code. The temperature and stress results of the unit cell(7HP) problem and the Minicore problem are presented and compared with reference data in steady and transient conditions to confirm the validity of the code coupling. At last, the summary of the study and recommendations are given in Chapter 5.

Chapter 2. Customization of OpenFOAM

Solid Mechanics Solver

To develop a high fidelity multi-physics simulation tool for heat pipe cooled reactor core under operation condition, the open source-based CFD code, OpenFOAM was modified. In this chapter, the description of the OpenFOAM solid mechanics solver and the modified solver, and the boundary condition would be illustrated.

2.1 Solid Mechanics Solver

2.1.1 solidDisplacementFoam

OpenFOAM provides a basic structural analysis solver named ‘solidDisplacementFoam’. This solver can analyze transient conditions with small stress deformation assuming linear elasticity. This solver can be used to calculate linear elasticity case in which small deformation occurs, as well as stress due to thermal expansion. In the case of the heat pipe cooled reactor core, the corresponding solver was selected because it is expected that the deformation will not be large under normal operating conditions (Sterbentz, et al., 2017).

The ‘solidDisplacementFoam’ solver calculates temperature and displacement using equations (2-1) and (2-2).

Momentum equation

$$\frac{\partial^2(\rho\mathbf{u})}{\partial t^2} = \nabla \cdot [(2\mu + \lambda)\nabla\mathbf{u}] + \nabla \cdot [\mu(\nabla\mathbf{u})^T + \lambda\mathbf{I}tr(\nabla\mathbf{u}) - (\mu + \lambda)\nabla\mathbf{u}] - \nabla(3K\alpha T) \quad (2-1)$$

where

- ρ = Density (kg/m³)
- u = Displacement (m)
- μ = Lamé's second coefficient (shear modulus) (Pa)
- λ = Lamé's first coefficient (K)
- \mathbf{I} = Unit tensor
- K = Bulk modulus (Pa)
- α = Thermal expansion coefficient (/K)
- T = Temperature (K)

Heat conduction equation

$$\rho c \frac{\partial T}{\partial t} = \nabla \cdot k\nabla T + q''' \quad (2-2)$$

where

- c = Specific heat capacity (J/kgK)
- k = Thermal conductivity (W/mK)
- q''' = Volumetric heat generation rate (W/m³)

In addition, the stress and strain could be calculated as equation (2-3) and (2-4) using displacement from equation (2-1).

Strain

$$\varepsilon = \frac{1}{2} [\nabla u + (\nabla u)^T] \quad (2-3)$$

Stress

$$\sigma = 2\mu\varepsilon + \lambda\text{tr}(\varepsilon)\mathbf{I} \quad (2-4)$$

2.1.2 Verification of the thermal-structural analysis solver

The OpenFOAM's thermal-structural analysis solver has only been verified against the simple examples in the OpenFOAM official user guide, and there has been no verification on thermal stress analysis in the situation where thermal analysis and structural analysis are performed simultaneously. Therefore, verification of the thermal stress solver was performed against the three kinds of problems. Among them, one problem was selected from the Autodesk Nastran verification manual (Autodesk, 2015) and the other two were selected from the ANSYS mechanical APDL verification manual. (ANSYS, 2013)

Thermal strain, displacement and stress on a heated beam

The first verification problem is the thermal expansion of a beam is described in figure 2.1. The problem is divided into case 1 that one end is constrained, and case 2 that both ends are constrained. The calculation result of displacement and strain were compared with an analytic solution for case 1, and the stress calculation result was compared for case 2. It is assumed that the temperature of the entire beam rises from a reference temperature of -50°C to 25°C . The

properties used in the calculation are shown in table 2.1. Since the reference temperature of OpenFOAM is set as 0°C, the beam temperature rose to 75°C instead of 25°C to maintain the same temperature difference.

The calculation results of the one end constrained case are presented in figure 2.2 and table 2.2. The calculation results of displacement and strain at the free end of the beam coincide well with the analytic solution. Although the strain was calculated correctly, there was an error in the displacement, because the calculated displacement value from the OpenFOAM is based on cell center data, meanwhile, the analytic solution is based on the point data.

In both end constrained case, the calculation results are described in table 2.3 and figure 2.3. Displacement does not occur in this case because both ends are constrained, and the stress calculation result in the x-axis direction is consistent with the analytic solution.

Table 2.1 Properties of heated beam problem

L (m)	A (m ²)	E (Pa)	ν	α (/K)
1	0.01	2.068e+11	0.3	1.2e-05

Table 2.2 Heated beam problem case 1 calculation results

Description	Analytic solution	OpenFOAM result	Error(%)
Beam free end displacement (m)	0.0009	0.00089	-1.1
Beam constrained end axial strain	0.0009	0.0009	0.0

Table 2.3 Heated beam problem case 2 calculation results

Description	Analytic solution	OpenFOAM result	Error
Beam constrained end axial stress(MPa)	-186	-186	0.0



Figure 2.1 Conceptual figure of the heated beam problem

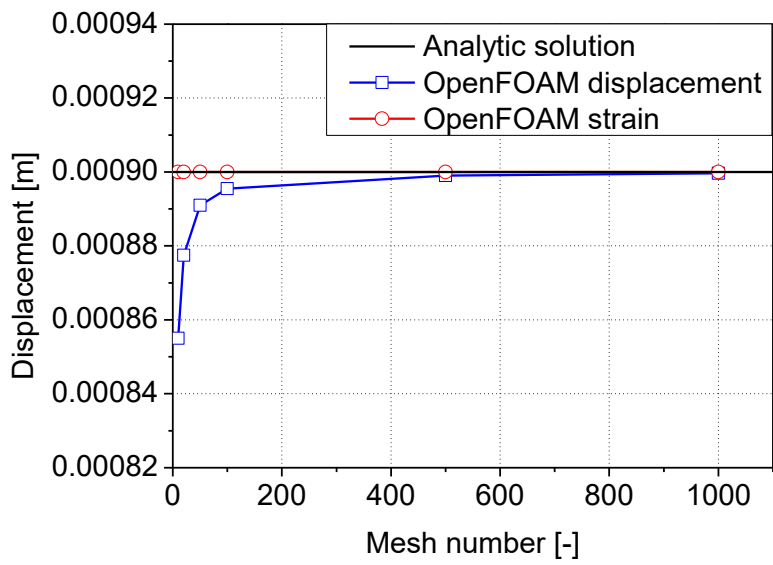


Figure 2.2 Displacement and strain result for case 1 of the heated beam problem

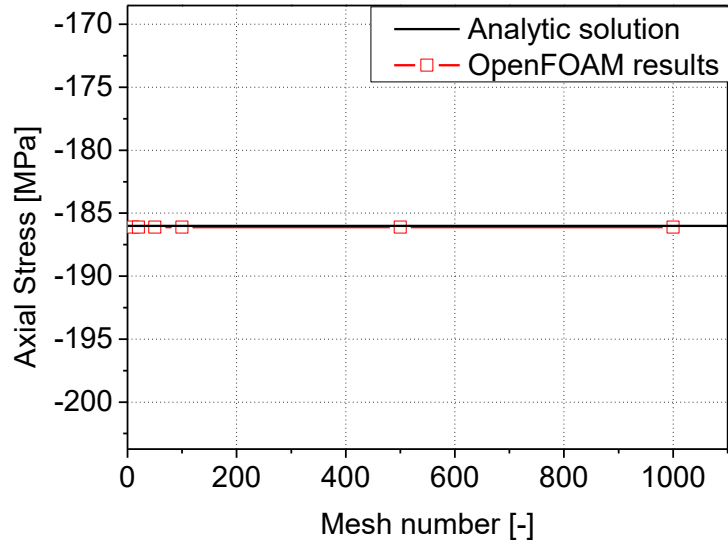


Figure 2.3 Axial stress result for case 2 of the heated beam problem

Thermal stresses in a long cylinder

The second problem is the steady-state thermal stress calculation of the cylinder, while the temperatures of the inner and outer surfaces are constant. The inner surface temperature is -1°C and the outer surface temperature is 0°C . Similar to the first problem, the inner surface temperature was set as 0°C and the outer surface temperature was set as 1°C , considering that the reference temperature of OpenFOAM is 0°C . The geometry is shown in figure 2.4, and material property information used in the calculation is shown in table 2.4.

Figure 2.5 shows the temperature profile of the cylinder in the radial direction. The OpenFOAM calculation result coincides well with the analytic solution. Figure 2.6 and figure 2.7 show the axial and tangential stress at the inner surface and outer surface of the cylinder. As the number of meshes increases, the OpenFOAM calculation result approaches the analytic solution, and the mesh convergence is confirmed. The results indicate that present stress analysis solver of the OpenFOAM is applicable for stress calculations.

Table 2.4 Properties of steady-state cylinder problem

a (m)	b (m)	k (W/mK)	E (Pa)	ν	α (/K)
0.0047625m	0.015875m	43.51	2.068e+11	0.3	1.44e-05

Table 2.5 Calculation results for steady-state cylinder problem

Description	Analytic solution	OpenFOAM result	Error(%)
Temp. at $x=0.00708$ m ($^{\circ}\text{C}$)	0.3296	0.3312	0.48
Axial stress at $r=a$ (MPa)	2.899	2.884	-0.52
Tangential stress at $r=a$ (MPa)	2.899	2.841	-2.00
Axial stress at $r=b$ (MPa)	-1.342	-1.344	0.15
Tangential stress at $r=b$ (MPa)	-1.342	-1.337	-0.37

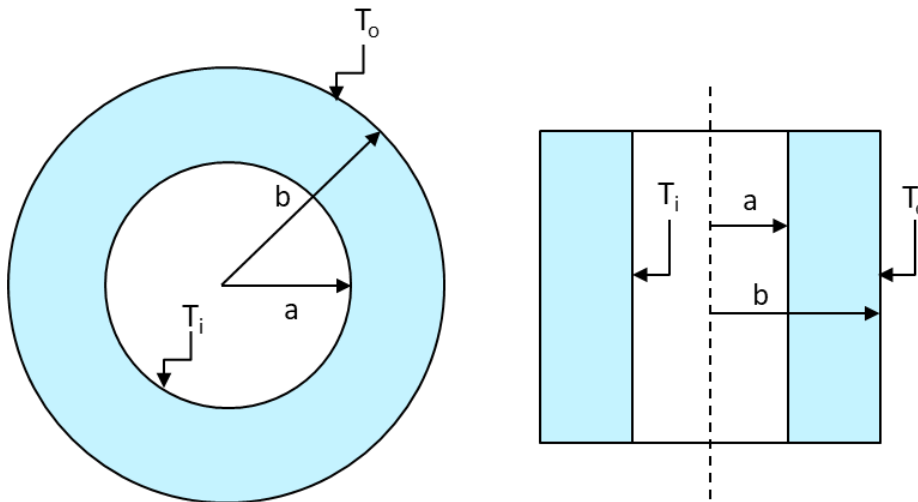


Figure 2.4 Conceptual figure of the steady-state cylinder problem

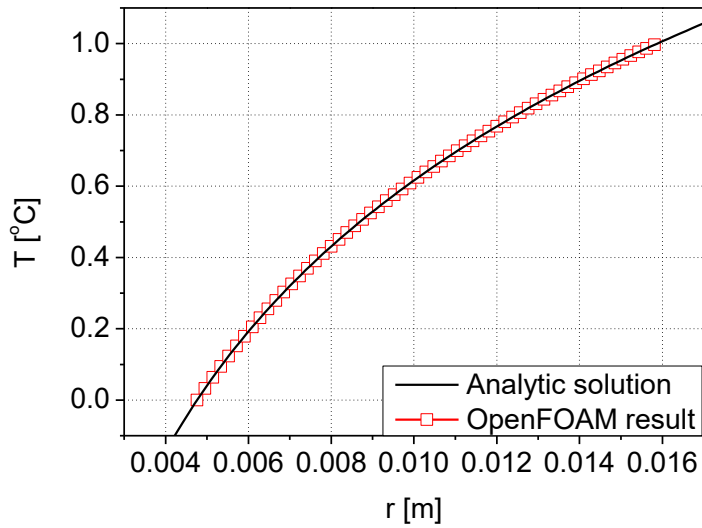


Figure 2.5 Temperature distribution result of the steady-state cylinder problem

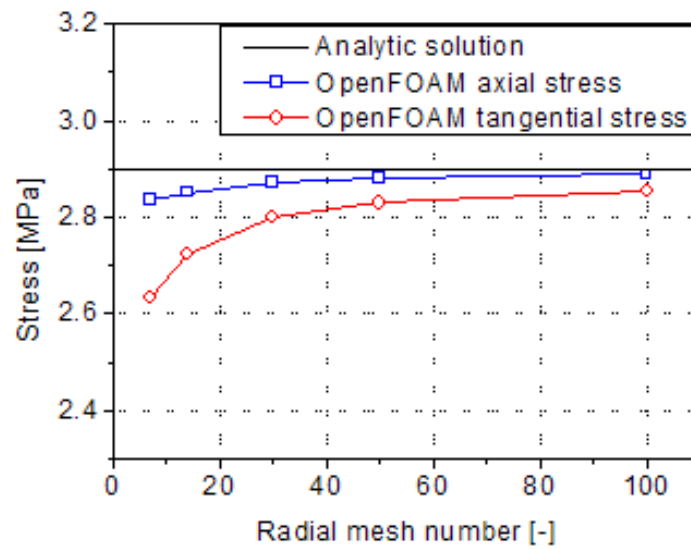


Figure 2.6 Inner surface stress result of the steady-state cylinder problem

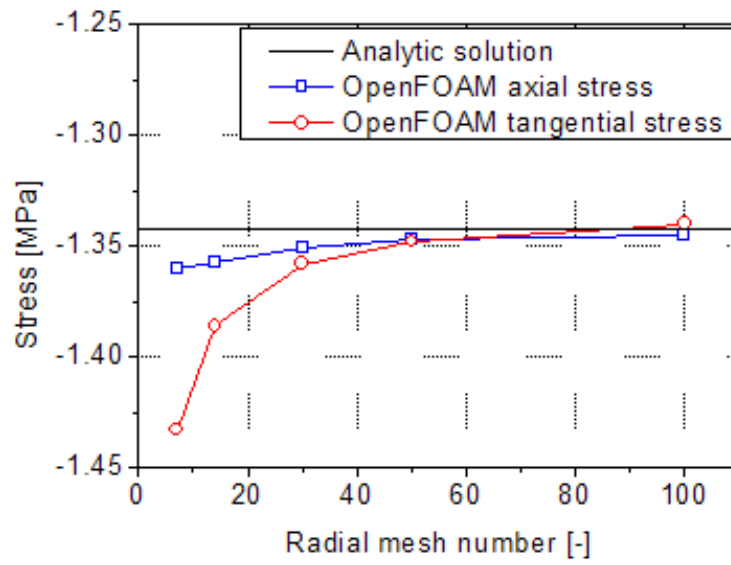


Figure 2.7 Outer surface stress result of the steady-state cylinder problem

Transient thermal stresses in a cylinder

The third problem is the transient calculation of thermal stress of the cylinder, where the temperature of the outer surface increases with time. The initial temperature of the cylinder is 21.11°C , and the temperature of the outer surface is $T_f(t) = 21.11 + 0.55t^{\circ}\text{C}$. Similar to the previous problem, considering that the reference temperature of the OpenFOAM is 0°C , the initial temperature of the cylinder was set to 0°C and the temperature of the outer surface was set to $T_f(t) = 0.55t^{\circ}\text{C}$. The boundary condition of inner surface was set as adiabatic. The geometry is shown in figure 2.8, and material property information used in the calculation is shown in table 2.6.

Figure 2.9 shows the inner-outer surface temperature difference calculated by ANSYS and OpenFOAM. This result provides the consistency of the OpenFOAM result with the reference ANSYS result. The figure 2.10 and 2.11 show the stress calculation results of the inner surface and the outer surface of the cylinder at $t=420$ sec. Similar to the steady-state problem, mesh convergence was confirmed and through the three verification problems, the thermal-structural analysis solver of the OpenFOAM was verified.

Table 2.6 Properties of transient cylinder problem

a (m)	b (m)	h (m)	ρ (kg/m ³)	
0.0254	0.0762	0.508	7861	
k (W/mK)	c (J/kgK)	E (Pa)	ν	α (/K)
43.51	418.68	2.068e+11	0.3	1.512e-05

Table 2.7 Calculation results of transient cylinder problem

Description	Analytic solution	OpenFOAM result	Error(%)
Temp. difference (°C)	36.67	36.55	-0.33
Tangential stress at r=a (MPa)	71.3	69.615	-2.36
Tangential stress at r=b (MPa)	-92.3	-92.693	0.43

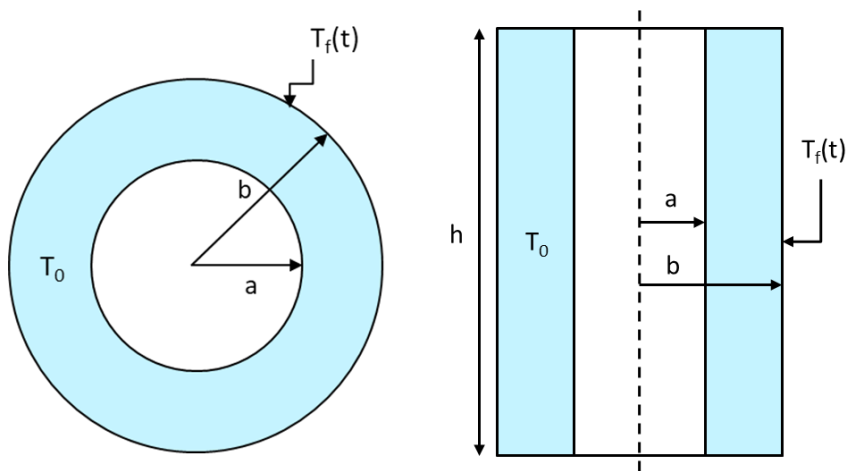


Figure 2.8 Conceptual figure of the transient cylinder problem

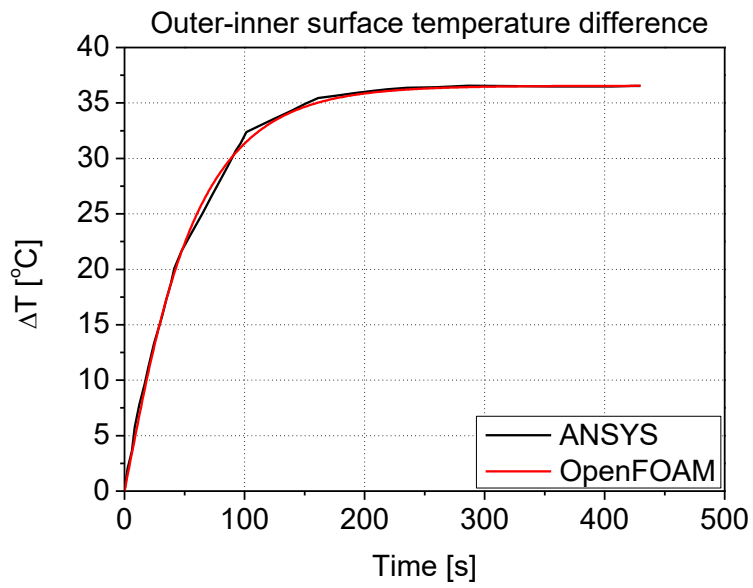


Figure 2.9 Inner-outer surface temperature difference of the transient cylinder problem

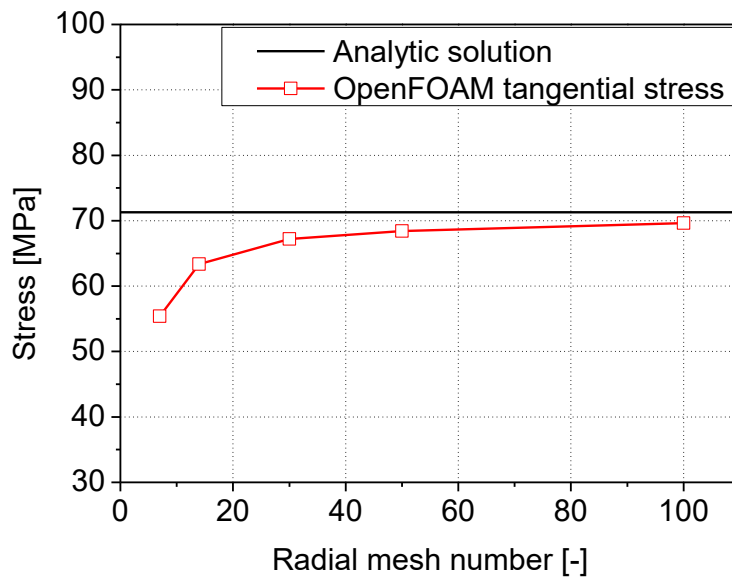


Figure 2.10 Inner surface stress result of the transient cylinder problem

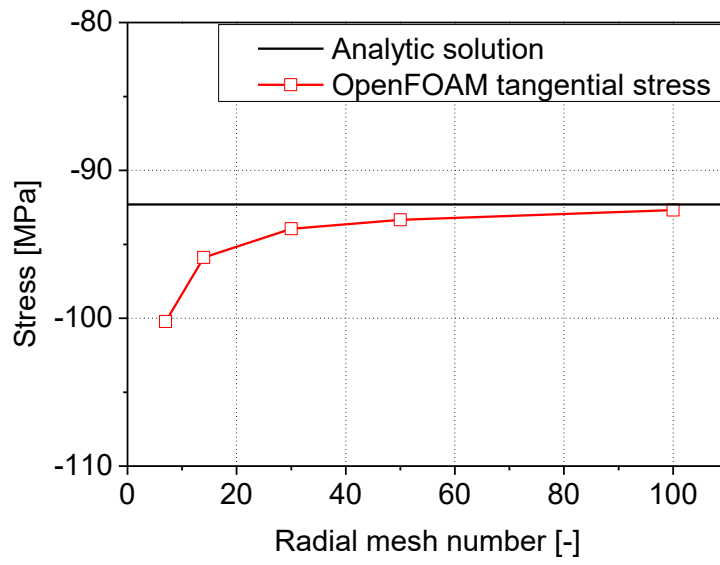


Figure 2.11 Outer surface stress result of the transient cylinder problem

2.2 Solver Customization

For the code coupling between OpenFOAM and ANLTHP, the OpenFOAM's thermal-structural analysis solver has been improved, and a new boundary condition for external data exchange has been added to the OpenFOAM.

2.2.1 Modification of the solver

OpenFOAM's basic thermal-structural analysis solver has some limitations. One of them is that it can calculate only for a single material case and constant material properties. However, the heat pipe cooled reactor core consists of a few materials: heat pipe, monolith, and nuclear fuel. In addition, the material properties of each material vary with temperature. For the accurate core analysis, the new solver was defined by modifying the basic thermal-structural analysis solver of the OpenFOAM to consider the change in material properties according to the type of material and temperature.

First, the scalar field named 'material' that contains composition information for each cell was newly defined so that the physical properties of each material can be applied respectively. In the solver, according to the 'material' value of each cell, different thermal and mechanical properties are used for the calculation. In this process, the material properties used as a constant in the original solver have been modified to be used as a function of temperature. In addition, for the coupling with the neutronics code, which is planned as a future work, the scalar field named 'qvoldat' which contains volumetric heat of each cell was additionally defined. These modifications of the solver are summarized in table 2.8.

In order to check whether the modifications of the OpenFOAM solver were properly reflected, the analysis of the single nuclear fuel rod problem was conducted. The geometry is described in figure 2.12 and the volumetric heat generation and property of UO_2 were applied. The calculation result was illustrated in figure 2.13, and the OpenFOAM calculation result matched well with the analytic solution.

Table 2.8 Modification of OpenFOAM solid mechanics solver

Solver	Original solver	Customized solver
Material type	Single material	Multiple materials
Material property	Constant	Function of temperature
Data fields import	x	Material type and volumetric heat

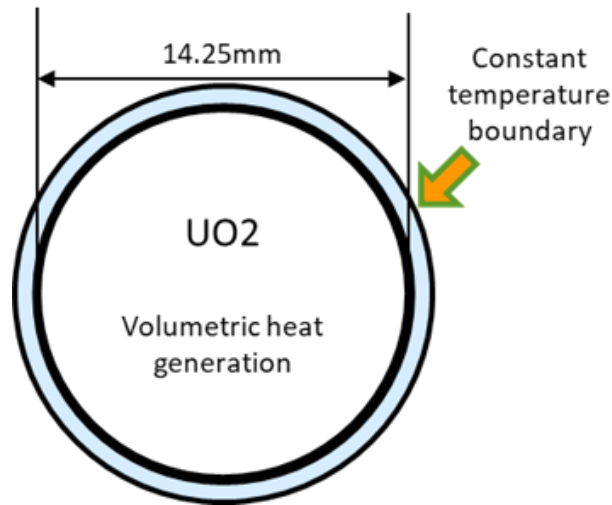


Figure 2.12 The geometry of UO₂ single rod problem

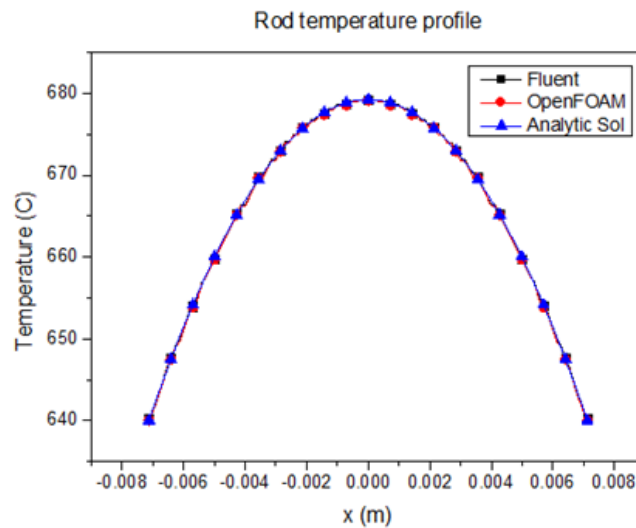


Figure 2.13 The calculation result of UO₂ single rod problem

2.2.2 Boundary condition for external coupling

The OpenFOAM provides a file-based data input/output system, which can be designated as a boundary condition. There are external data exchange boundary conditions named ‘externalCoupledTemperature’ and ‘externalWallHeatFluxTemperature’ for thermal analysis. However, these boundary conditions are available only for liquids and cannot be used on solid surfaces. Therefore, for the coupling analysis of the heat pipe cooled reactor core, externalCoupledTemperature boundary condition was modified to define a new boundary condition called ‘externalCoupledTemperatureSolid’. Using the externalCoupledTemperature’s source file, the exchanged variables were modified to suit the solid surface. When using this new boundary condition, the OpenFOAM writes the boundary area, heat flux, and thermal properties of the solid surface to an external file, and reads the boundary temperature from the external file.

Chapter 3. Establishment of Code Coupling System

To develop a multi-physics core simulation tool, the coupling between the thermal-structural analysis code, OpenFOAM, and the heat pipe thermal analysis code, ANLHTP were performed. OpenFOAM and ANLHTP are externally coupled, and this chapter would describe ANLHTP and the coupling methodology using supervising Python code.

3.1 ANLHTP

ANLHTP is a one-dimensional heat pipe analysis code developed by ANL and could perform analysis on sodium heat pipe. ANLHTP uses a thermal resistance network to predict steady-state heat pipe performance and temperature. ANLHTP takes the wall temperature as an input and calculates the corresponding heat transfer rate. However, in the OpenFOAM-ANLHTP coupling system, OpenFOAM provides heat transfer rate and ANLHTP should calculate temperature to be used as the boundary condition of the OpenFOAM as shown in figure 3.2. Therefore, ANLHTP calculated temperature inversely from the given heat transfer rate, using the python code to be described later,

The geometric information including the diameter or wick structure of the heat pipe and thermal properties such as heat sink temperature is used in the ANLHTP

input. These heat pipe information are used to calculate the operation limit of the heat pipe and the temperature and heat transfer rate. Especially, for the calculation of the operation limit, geometric information of the heat pipe is used to determine the operation limit and the thermal property is used to check whether the operation limit is satisfied for a specific wall temperature.

The validation of ANLHTP was referenced from the previous research conducted by ANL (Lee, 2019). For the validation, heat transfer capability and operation limit of the sodium heat pipe were compared with experiment data (Chi, 1976) (Dunn and Reay, 1978). Figure 3.3 shows the validation results of the ANLHTP and the calculation results show good agreement with the experiment.

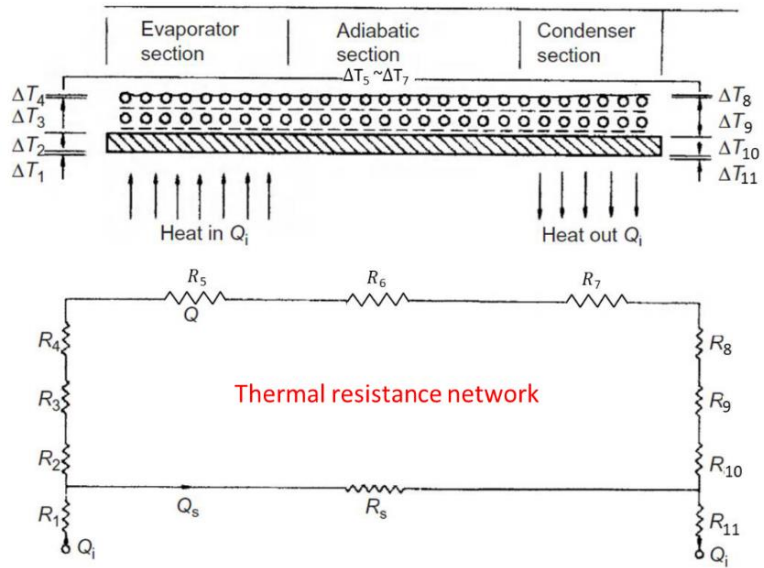


Figure 3.1 Thermal resistance network of ANLHTP (Lee, 2019)

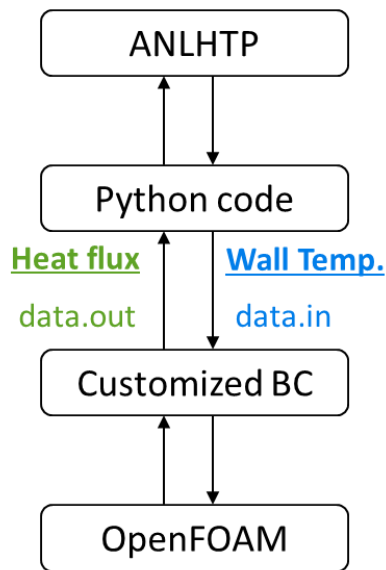
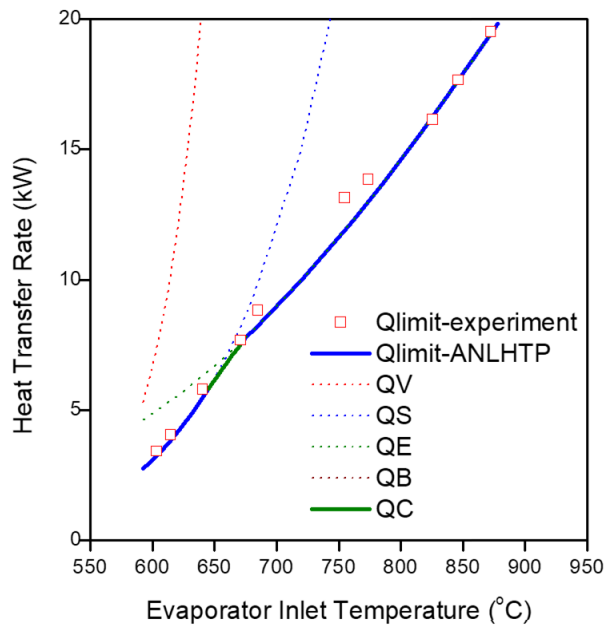
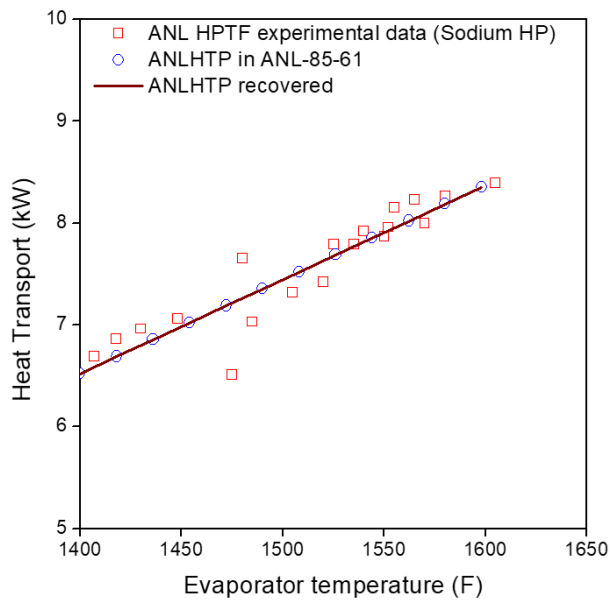


Figure 3.2 Schematic of coupling between OpenFOAM and ANLHTP



(a) LANL sodium heat pipe test simulation



(b) ANL HPTF test simulation

Figure 3.3 ANLHTP validation results (Lee, 2019)

3.2 Coupling Strategy

To analyze the heat pipe cooled reactor core, the OpenFOAM-ANLHTP coupled code should be capable of transient calculation. However, ANLHTP is a steady-state code.

Since ANLHTP calculates only one temperature without axial temperature distribution for each evaporator, adiabatic, and condenser section, the boundary wall temperature of the OpenFOAM is uniform in an axial direction. However, since there are an axial power and temperature distribution in reality, the uniform boundary wall temperature is not physically valid. Therefore, the wick-vapor interface inside the heat pipe, where the temperature is expected to be constant as the saturation temperature of the working fluid, is set as the data exchange position. Furthermore, with the 1D quasi-steady-state assuming for the heat pipe vapor core region (Zuo et al., 1998), it is available to use ANLHTP in the transient calculation. The heat pipe wick section and the outer wall section are calculated by OpenFOAM so that the axial temperature distribution can be reflected. During the coupling process, OpenFOAM provides the heat transfer rate at the wick-vapor interface, and ANLHTP calculates the corresponding wick-vapor interface temperature.

The coupling process was supervised with Python code to control the file-based data exchange between the OpenFOAM and the ANLHTP.

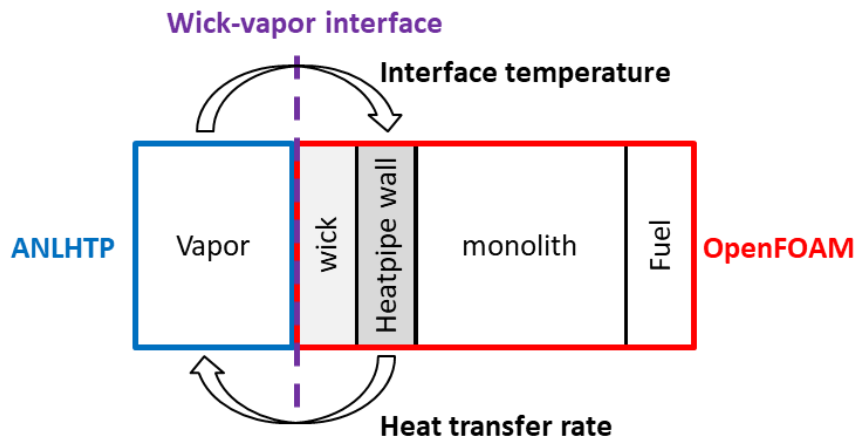


Figure 3.4 Schematic of data exchange at wick-vapor interface

3.2.1 Supervising python code

Python code has two main roles: Relaying the data exchange between OpenFOAM-ANLHTP, and executing ANLHTP. The OpenFOAM-ANLHTP coupling calculation procedure is shown in figure 3.5.

The operating procedure of the supervising Python code is as follows. First, create the OpenFOAM.lock file primitively. This is to perform the first timestep calculation of OpenFOAM, and then it checks whether the lock file exists. If the lock file exists, Python waits because the OpenFOAM calculation is still running. When the OpenFOAM calculation is done, the OpenFOAM writes data.out file containing the boundary area, heat flux, and thermal properties, and delete the lock file. If the lock file does not exist, the Python code read data.out file and import data from the file. Using the boundary area and heat flux, the total heat transfer rate for each boundary is calculated by the Python code.

Using the calculated heat transfer rate and the current OpenFOAM boundary temperature, a new boundary temperature corresponding to the heat transfer rate is calculated by ANLHTP. Next, the Python writes the calculated boundary temperature in the data.in file, and create the lock file to perform OpenFOAM calculation again.

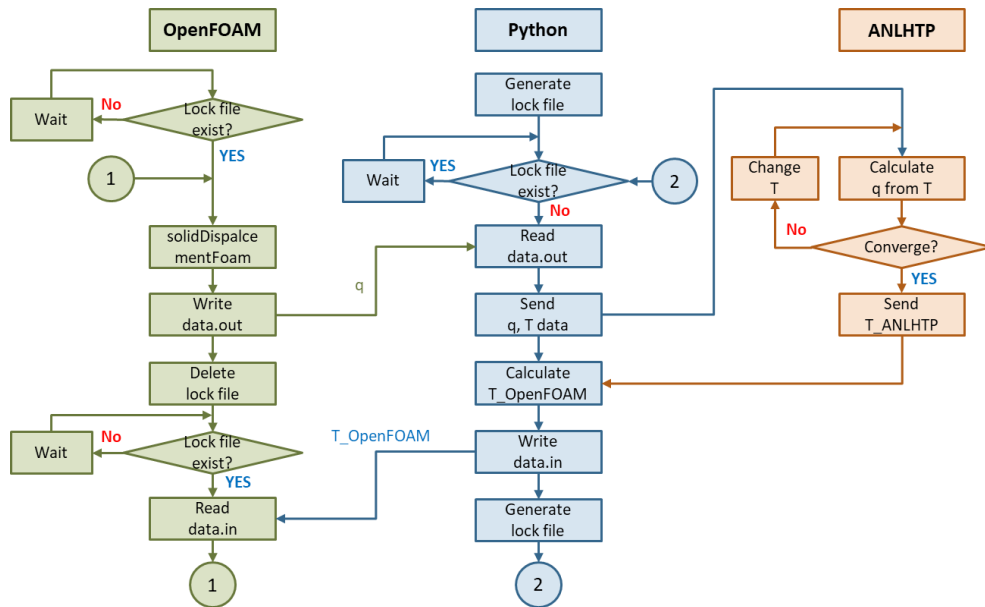


Figure 3.5 Flow chart of coupling procedures in OpenFOAM-ANLHTP

3.2.2 Interface temperature convergence strategy

To calculate the heat pipe boundary temperature from the given heat transfer rate using ANLHTP, an additional python script is implemented. The heat transfer rate and current OpenFOAM boundary temperature are entered into an additional python script, and in the range of the current boundary temperature $\pm 100^{\circ}\text{C}$, ANLHTP is executed until it finds the boundary temperature at which the corresponding heat transfer rate is calculated. To find the correct boundary temperature, iteration with the Newton-Raphson method is conducted.

Meanwhile, since the temperature calculated by ANLHTP is very sensitive to the heat transfer rate, if the calculated temperature is used as it is, the boundary temperature changes greatly and the calculation becomes unstable. Therefore, the boundary temperature was determined using different methods according to the steady and transient calculation conditions.

In order to converge the boundary temperature within one timestep, 10 outer iterations were performed in each OpenFOAM timestep, and the boundary temperature was converged during the corresponding outer iteration. For the steady-state calculation, the boundary temperature was determined using the fixed point (under-relaxation) method only once at the first iteration during 10 outer iterations. In contrast, for the transient calculation, the Picard iteration was used with the secant method and the fixed point method during 10 outer iterations. Specifically, the fixed point method was used at the first iteration, and the secant method was used to increase the convergence speed. When the temperature difference calculated in each iteration became smaller as it approached the solution, there was a problem that convergence was difficult with the secant method, so the fixed point method was used again. As a result, it can be confirmed

that boundary temperature converges through Picard iteration within one time step as shown in figure 3.6.

Fixed point method (under-relaxation)

$$T_{n+1} = \omega \cdot T_n + (1 - \omega) \cdot T_{anlhtp_n} \quad (3-1)$$

where

T_n = OpenFOAM's boundary temperature at n-th step (K)

ω = Relaxation factor

T_{anlhtp_n} = ANLHTP's boundary temperature at n-th step (K)

Secant method

$$T_{n+1} = T_n - \frac{T_n - T_{n-1}}{FQ_n - FQ_{n-1}} FQ_{n-1} \quad (3-2)$$

where

FQ_n = $T_n - T_{anlhtp_n}$ (K)

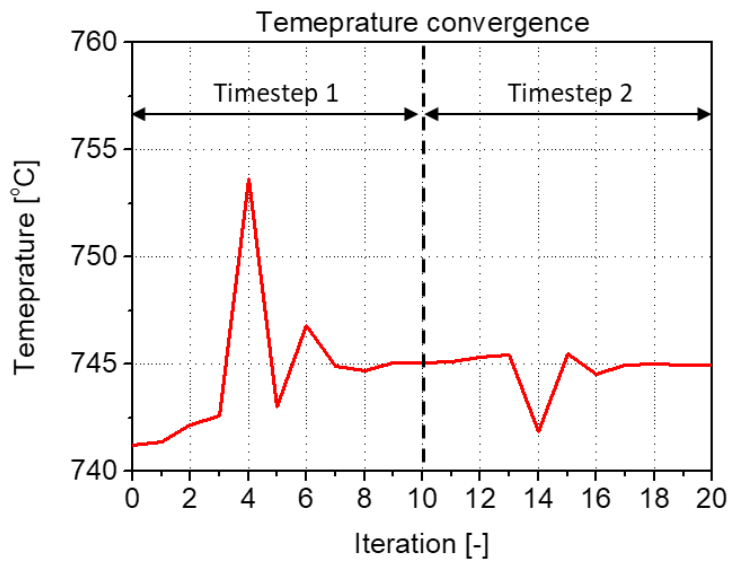


Figure 3.6 Boundary temperature convergence during transient calculation

Chapter 4. Demonstration of the Coupled OpenFOAM-ANLHTP Code

After the OpenFOAM-ANLHTP code system was established, the simulations for the heat pipe cooled reactor core was performed to demonstrate the application of a coupled code system.

For the demonstration of the OpenFOAM-ANLHTP coupled code, the steady-state and transient analyses were conducted for the unit cell(7HP) problem and the Minicore problem. For both unit cell and Minicore problems, the thermal-structural analysis results were evaluated with comparison to the PIRT analysis performed by INL.

4.1 Unit Cell (7HP) Problem

4.1.1 Problem specifications and modeling

The unit cell problem is the core with 6 fuel rods and 7 heat pipes. Its height and width are 1.5m and 0.048m respectively, and the geometry is shown in figure 4.1. Each fuel rod generates 2350W of heat and the power density of the core is 4.7W/cc. There is a helium gap between the fuel rod and the SS316 monolith. Whereas the actual MegaPower design uses a potassium heat pipe, the unit cell problem is calculated with a sodium heat pipe because the ANLHTP can only

calculate the sodium heat pipe. The other details of the design are described in table 4.1, and the 3D view of the mesh is described in figure 4.2.

The gap conductance model used in thermal analysis is the following modified Ross and Stoute Model. Since all cells are calculated as solids regardless of actual phase for the structural analysis, the stress and displacement are not calculated properly when there is a gap. Therefore, for the structural analysis was conducted only for the monolith region by removing the fuel rod, gap, and wick regions. The temperature results from the thermal analysis were used, and the material properties used are shown in Table 4.2.

Modified Ross and Stoute Model

$$h_f = \frac{k_g}{1.5(R_1 + R_2) + t_g + g} \quad (4-1)$$

$$\frac{1}{g} = \sum_i \left[\frac{y_i}{(g_o)_i} \right] \left(\frac{T_g}{273} \right)^{s+1/2} \left(\frac{0.101}{P_g} \right) \quad (4-2)$$

where

- h_f = Conductance through the gas in the gap (W/m²K)
- k_g = Thermal conductivity of gas (W/m K)
- R_1, R_2 = Surface roughnesses of the fuel and the sheath (m)
- t_g = Circumferentially averaged fuel-sheath gap width (m)
- g = Temperature jump distance (m)
- y_i = Mole fraction of i-th component of gas
- g_o = Temperature jump distance of i-th component of gas at STP (m)

- T_g = Gas temperature in the fuel-sheath gap (K)
- P_g = Gas pressure in the fuel-sheath gap (MPa)
- s = exponent dependent on gas type

A wire mesh screen wick heat pipe has been selected for the calculation and its working fluid is sodium. The detailed information on heat pipe is described in table 4.3. In the OpenFOAM-ANLHTP coupling system, the heat pipe wick and outer wall are included in the OpenFOAM mesh as shown in figure 4.3, as ANLHTP calculates the wick-vapor interface temperature. The heat sink temperature of the ANLHTP has referred to the temperature in the heat pipe cooled reactor system. (McClure et al., 2020)

Table 4.1 Geometric information of unit cell problem

Fuel rod outer diameter	1.412 cm
Helium gap thickness	0.0065 cm
Fuel-to-fuel pitch	1.60 cm
Fuel-to-HP-pitch	1.60 cm
HP hole diameter	1.575 cm
HP-to-HP pitch	2.7713 cm
Web thickness between HP-to-fuel holes	0.100 cm
Web thickness between fuel-to-fuel holes	0.175 cm

Table 4.2 Material properties of the heat pipe cooled reactor core

	ρ [kg/m ³]	Cp [J/kgK]	k [W/mK]	E [Pa]	ν	α [/K]
SS316	7500	640	16	1.4×10^{11}	0.265	2.0×10^{-5}
UO ₂	10970	320	3.2			
Wick	3223.24	645.6	43.51			

Table 4.3 Information of the sodium heat pipe

Wick type	Screen wick + artery
Container and screen wick material	SS304
Container OD	15.75mm
Container ID	14.75mm
Artery diameter	3.18mm
Number of turns	2
Number of artery	1
Mesh wire count	400
Mesh wire diameter	25 μ m
Space between wires	38.5 μ m

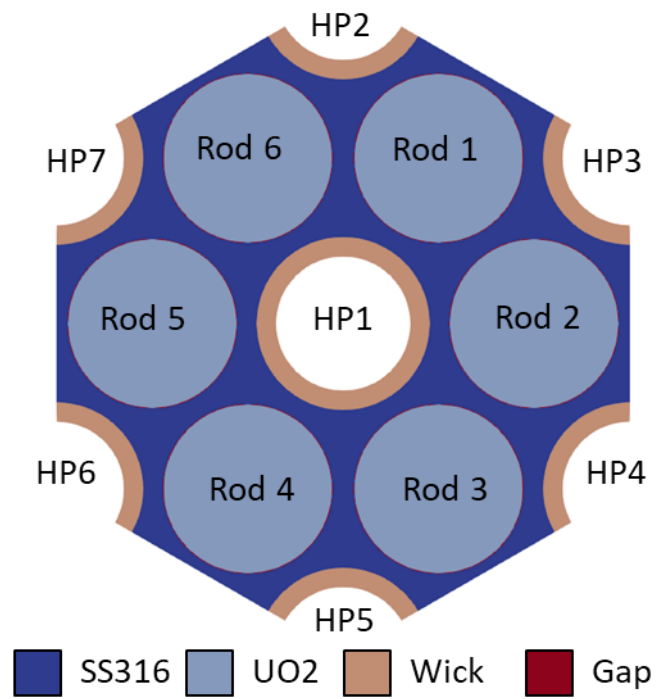


Figure 4.1 Schematic of the unit cell

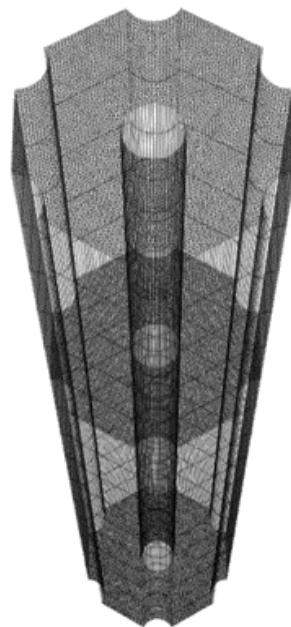


Figure 4.2 3D view of unit cell calculation mesh

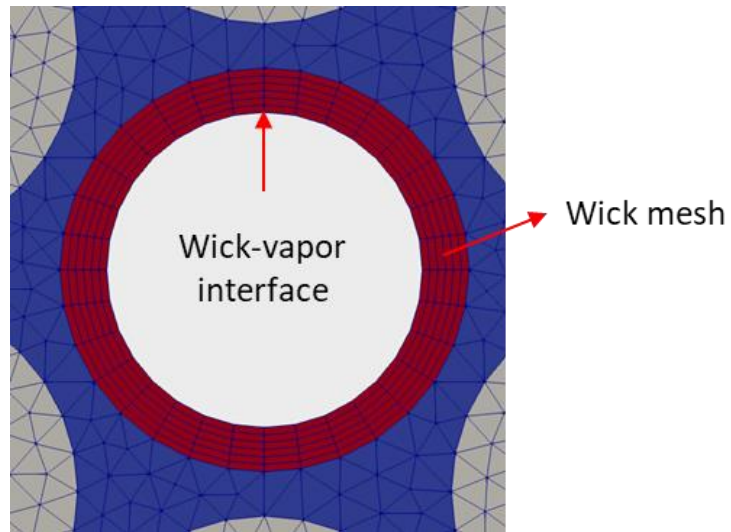


Figure 4.3 Calculation mesh of the heat pipe wick in OpenFOAM

4.1.2 Calculation results

For the thermal analysis, the heat pipe wick-vapor interfaces were coupled with ANLHTP, and all remain boundaries are set as an adiabatic condition. For the stress analysis, all boundaries are set as a zero traction force (free expansion).

Steady-state calculation

The calculation results of the thermal analysis are shown in figure 4.4 and figure 4.5. The peak fuel temperature is 811°C and the heat pipe boundary temperature is 741.1°C. The boundary temperature decreases at the beginning of the calculation and converges after several time steps. This is because there is no heat transfer at the boundary at the beginning of the calculation due to the same initial temperature. In addition, the stress analysis with the fixed bottom wall condition was simply performed simultaneously with thermal analysis to ensure that physical phenomena are properly reflected. Except for the abnormal calculation of the stress affected by the gap, figure 4.6 shows the displacement result that the thermal expansion is dominant in the axial direction.

The stress analysis is performed after removing some structures as shown in figure 4.7. The stress was calculated using the previous thermal analysis results. Figure 4.8 shows the monolith temperature distribution, displacement vector, and thermal stress results. The thermal expansion heading outward on the mid-plane can be confirmed by the displacement vector. This displacement result can be used to calculate the density change due to the volume expansion. As shown in figure 4.9, volume expansion can be calculated from the displacement result. The thermal stress has a peak value in a narrow web area between fuel rods and shows

about 30 MPa.

Transient calculation

The transient calculation was performed based on the assumption that the power of fuel rod No.1 increases 1.5 times. The restart calculation was performed using the previous steady calculation result, and other calculation conditions are the same as the steady calculation.

The thermal analysis results are shown in figure 4.10 and figure 4.11. As the power of fuel rod No.1 increases, the temperature of fuel rod No.1 increases to 881°C, and the boundary temperature of the heat pipes are increases. The boundary temperature of the heat pipes were calculated higher in the order close to fuel rod No.1 and symmetrical results were shown according to the distance from fuel rod No.1. It was qualitatively confirmed that the OpenFOAM-ANLHTP code coupling was properly performed.

Figure 4.12 shows the monolith temperature distribution and thermal stress in the transient calculation. The thermal stress induced by the temperature gradient increases as the monolith temperature around fuel rod No.1 increases. Especially, the maximum stress was 110MPa, which was more than three times larger than the ASME maximum allowable stress of SS316.

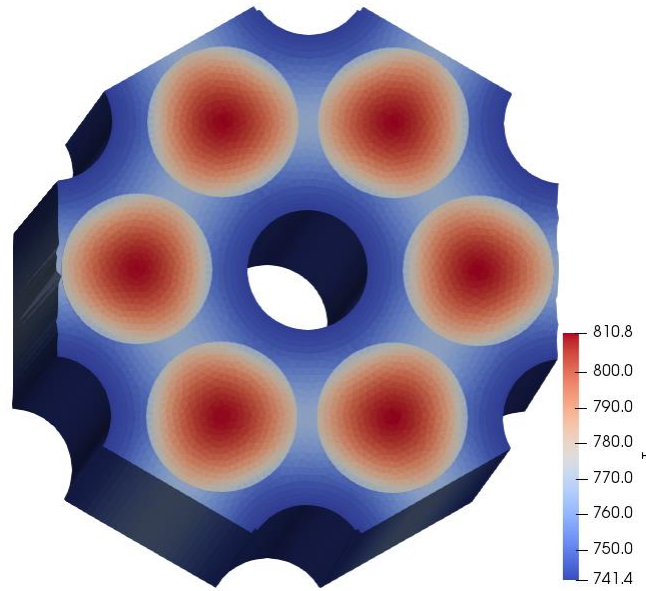


Figure 4.4 Thermal analysis result of unit cell in the steady-state calculation

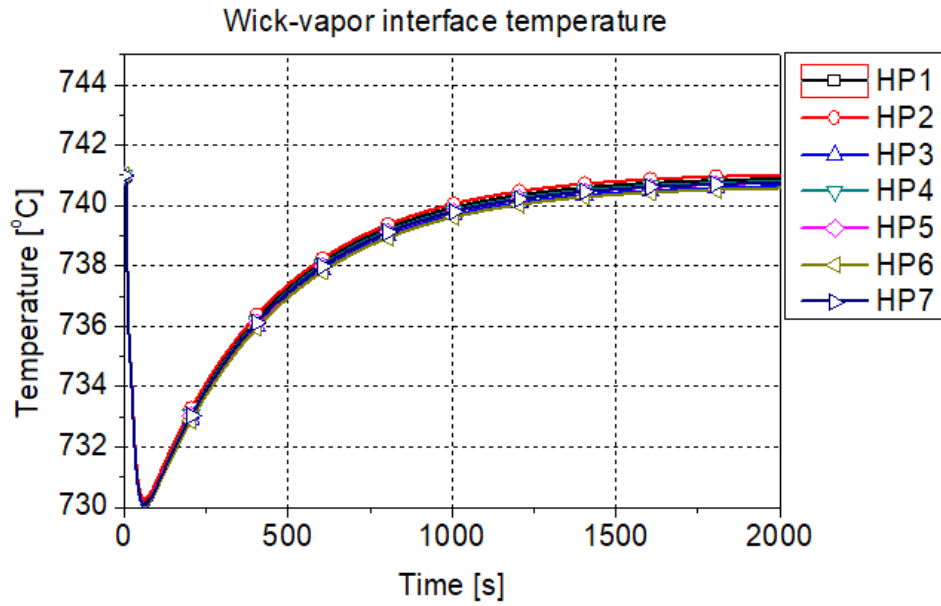


Figure 4.5 Boundary temperature of HPs in the steady-state calculation

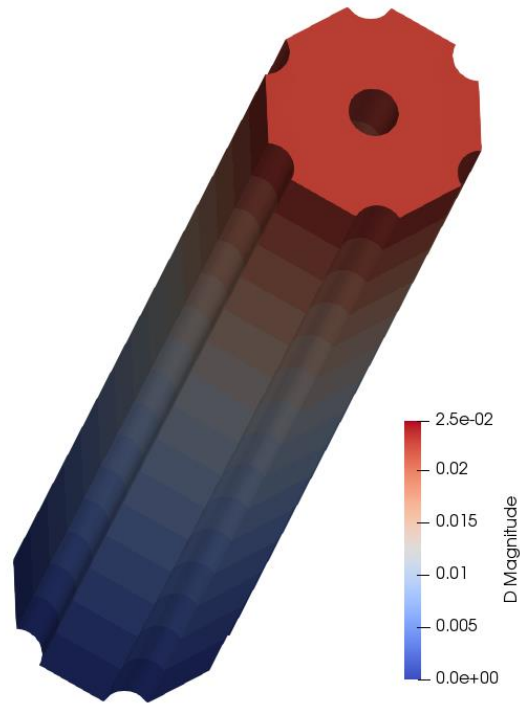


Figure 4.6 Displacement result of unit cell in the steady-state calculation

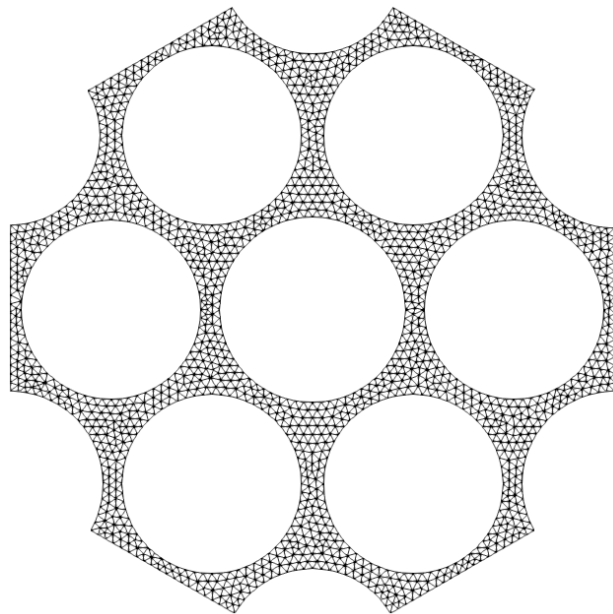


Figure 4.7 Calculation mesh of unit cell for stress analysis

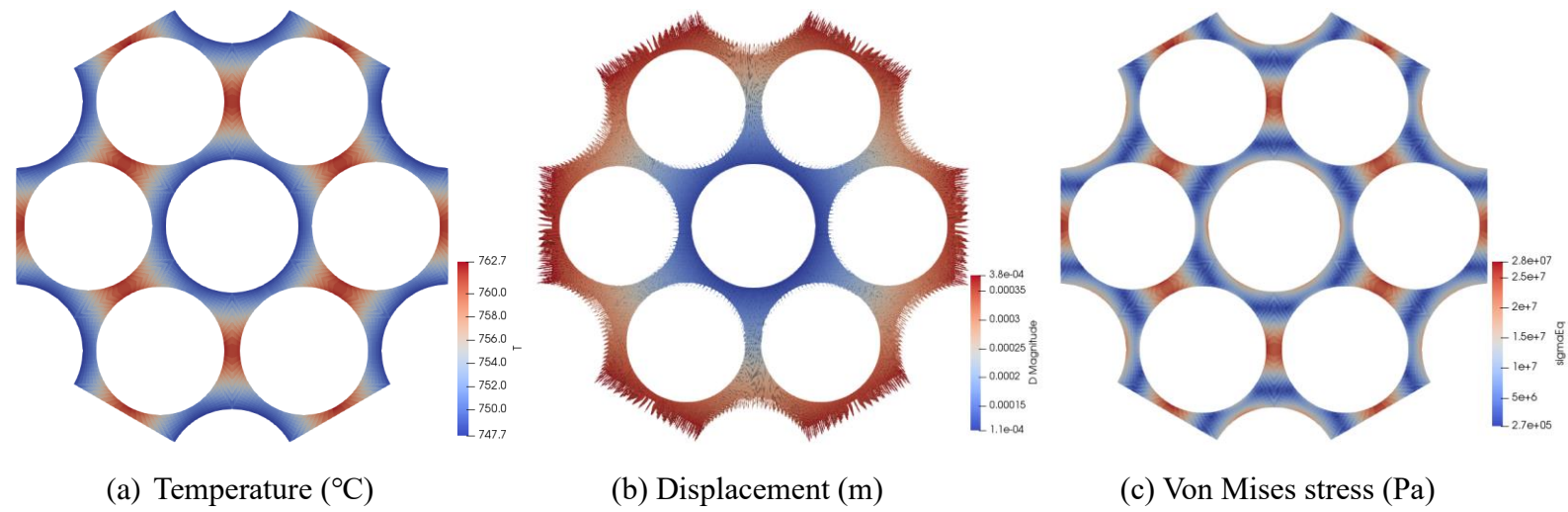


Figure 4.8 Stress analysis result of unit cell in steady-state calculation

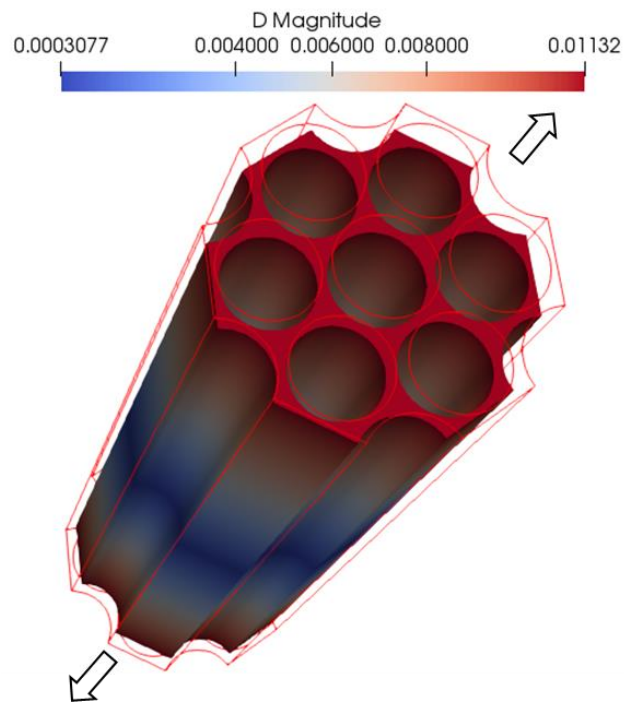


Figure 4.9 Volume expansion of unit cell in steady-state calculation (expanded volume was distorted for visibility)

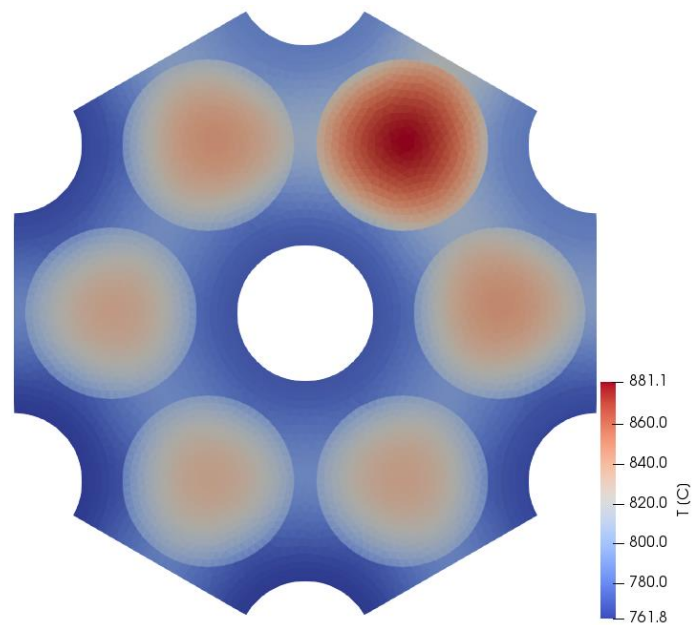


Figure 4.10 Thermal analysis result of unit cell in transient calculation

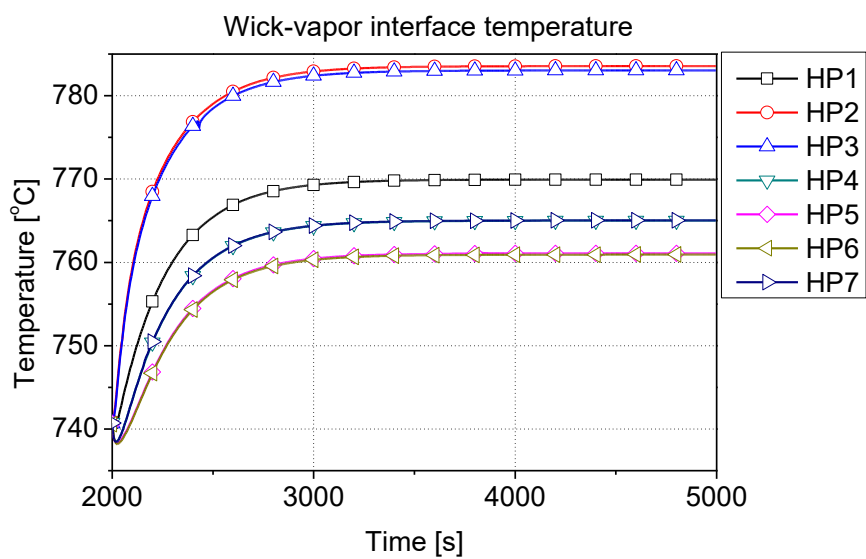


Figure 4.11 Boundary temperature of HPs in transient calculation

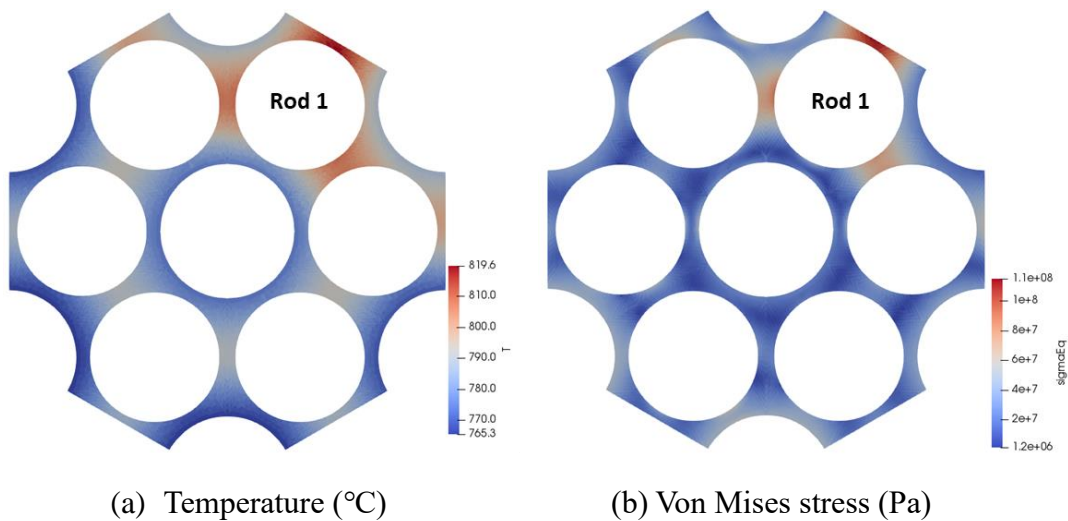


Figure 4.12 Monolith temperature and stress analysis results of unit cell in transient calculation

4.1.3 Comparison with reference data

The comparison between the OpenFOAM-ANLHTP coupled simulation result and MegaPower thermal-structural analysis results by INL was performed. (Sterbentz et al., 2017)

INL conducted a thermal analysis for the steady-state and the transient condition. A constant temperature boundary condition of 677°C was used for steady-state calculation on the heat pipe boundaries, and an adiabatic boundary was set for the failed heat pipe. The power distribution of fuel rods was provided from the neutronics analysis. The structural model takes the temperatures from the thermal models as input and assumes an initial temperature of 27°C. The bottom surface of the reactor is fixed and axial thermal expansions are measured from this fixed bottom surface and radial expansions are measured outward from the inner surface

The results of the steady-state thermal-structural analysis performed by INL are shown in figure 4.13. In the case of thermal analysis, it is hard to compare the results directly because the working fluid of the heat pipe and the power distribution of the fuel rods are different. The structural analysis result can be compared, unlike the thermal analysis, because the thermal stress is affected by temperature gradient rather than temperature itself. As shown in figure 4.14, the stress result of OpenFOAM-ANLHTP is comparable with the result of INL.

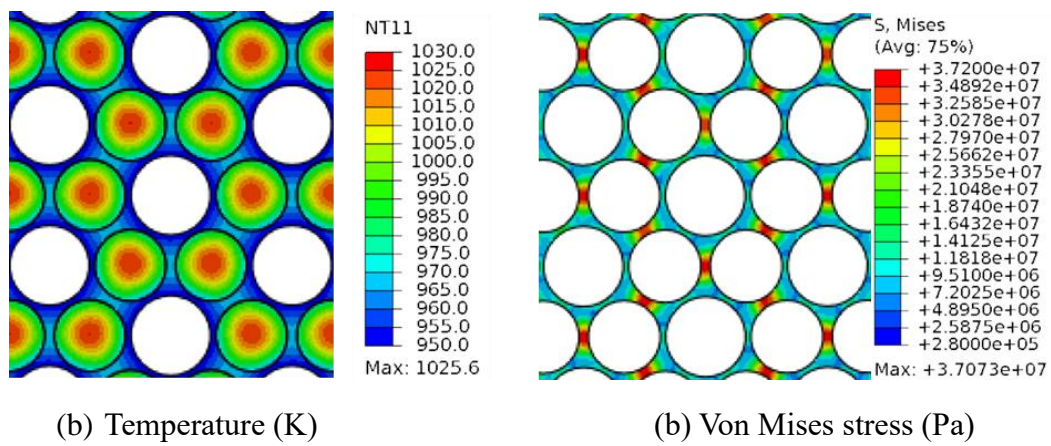


Figure 4.13 Thermal-structural analysis results of the MegaPower reactor core (Sterbentz et al., 2017)

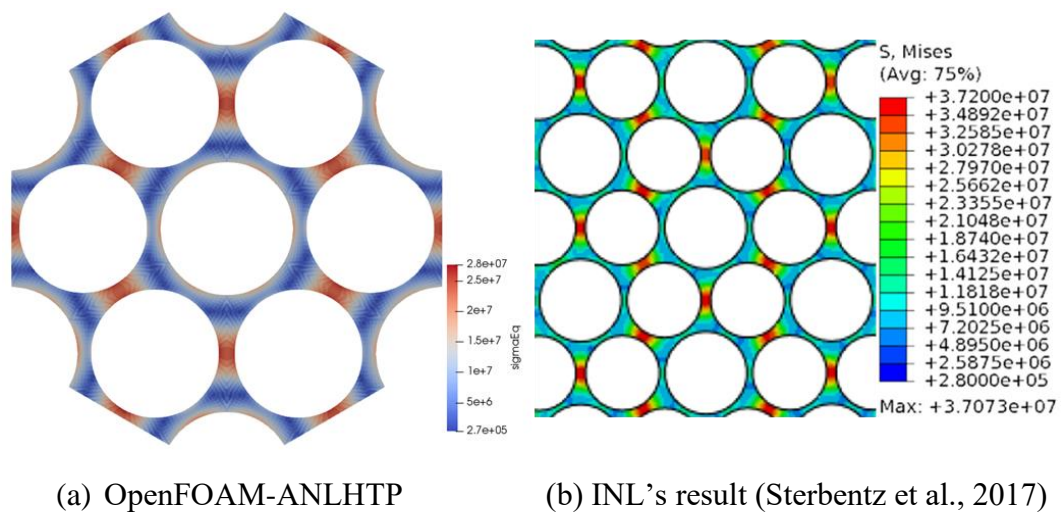


Figure 4.14 Monolith temperature and stress analysis results of unit cell in transient calculation

4.2 Minicore Problem

Following the unit cell problem, the analysis for the Minicore problem was conducted. The Minicore problem was designed by ANL to analyze the simplified heat pipe cooled reactor core using thermal-neutronics coupling code.

4.2.1 Problem specifications and modeling

Minicore is a 1m height and 0.3m width core containing 84 fuel rods and 55 heat pipes. Its shape is as shown in figure 4.15. The geometric information is all the same as that of the unit cell as shown in table 4.1. The heat generation rate of each fuel rod is 1578W and the power density is 4.7W/cc. All the other calculation conditions and methods are the same as for the unit cell problem and the 3D view of the mesh is described in figure 4.16.

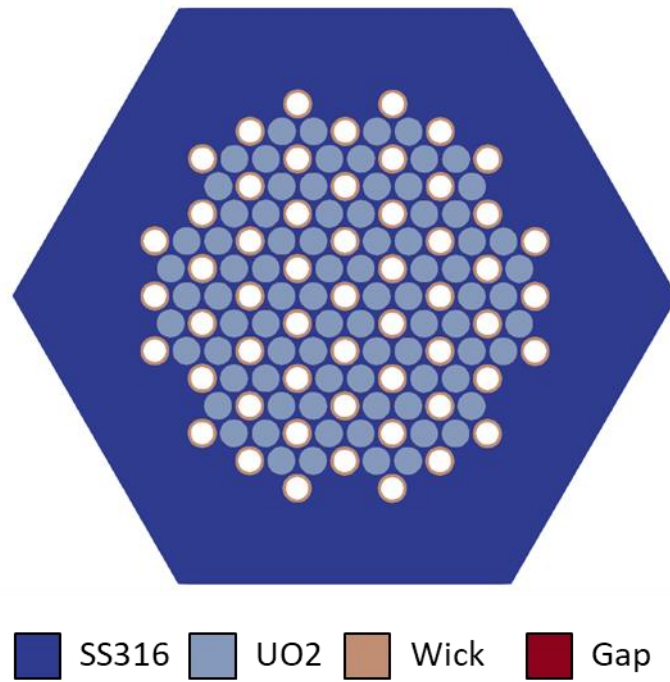


Figure 4.15 Schematic of the Minicore

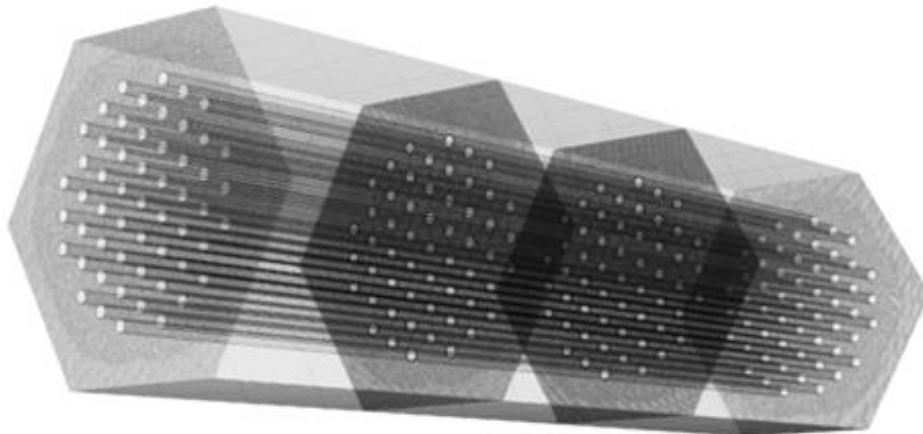


Figure 4.16 3D view of Minicore mesh

4.2.2 Calculation results

Steady-state calculation

Figure 4.17 shows the result of OpenFOAM standalone calculation with the constant heat pipe boundary temperature condition and OpenFOAM-ANLHTP coupled calculation. The coupled calculation result shows that the heat removal rate and boundary temperature are different according to the heat pipe position as shown in figure 4.18 and figure 4.19, unlike the constant temperature calculation. Specifically, the closer to the center of the core, the higher the heat removal rate and the boundary temperature of the heat pipe. This phenomenon cannot be seen at the constant temperature boundary calculation, the realistic physical phenomenon can be well reflected through the coupling analysis. The maximum temperature of the monolith is about 671 °C in the steady-state calculation, which is lower than the ASME limit of 820 °C.

Figure 4.20 and figure 4.21 show the stress analysis results of the Minicore. Each figure shows the result of the constant temperature boundary case and the coupling calculation case, and the maximum stress of 73 MPa and 230 MPa are calculated, respectively, exceeding the ASME maximum allowable stress of 29.6 MPa. This is because the suggested Minicore design was aimed for the thermal-neutronics calculation and stress analysis was not considered. Same with the unit cell problem, the volume expansion can be calculated from the displacement result as shown in figure 4.22. By comparing the stress analysis results for the constant temperature boundary condition and the coupling case, the difference in the temperature distribution of the monolith induces a significant difference in the stress.

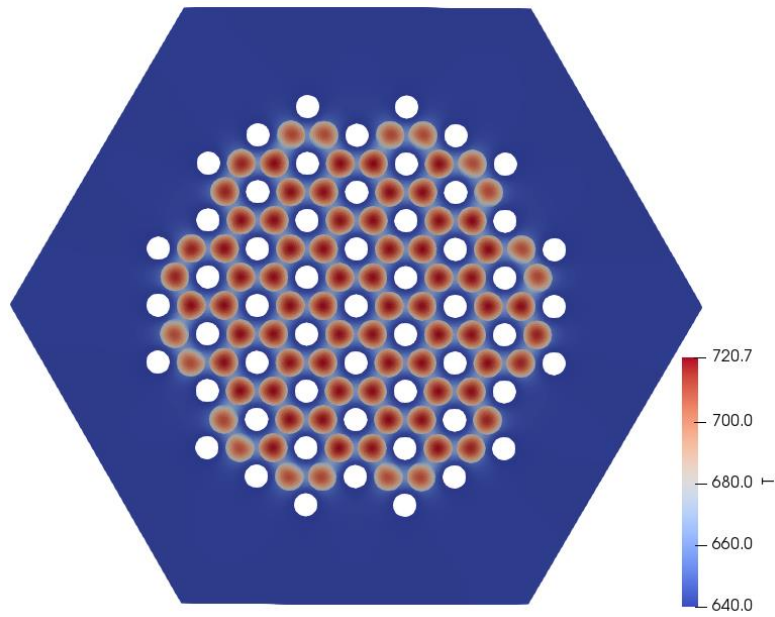
Transient calculation

The thermal analysis and stress analysis were performed for the transient heat pipe failed scenario. Specifically, one heat pipe failed scenario was simulated and the scenario was divided into the peripheral heat pipe failure scenario and the central heat pipe failure scenario. The figure 4.23 and 4.27 show the failed heat pipe of each scenario. The restart calculation was performed from the steady-state calculation result, and the boundary condition of the failed heat pipe was set as adiabatic assuming the worst case in which heat was not removed at all.

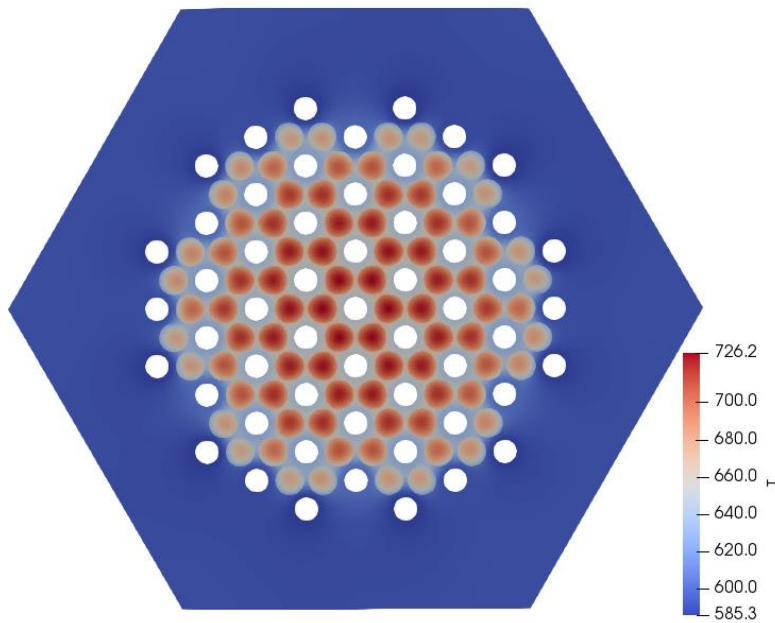
Figure 4.24 and figure 4.25 show the thermal analysis results of the peripheral heat pipe failure scenario, and figure 4.28 and figure 4.29 show the results of the central heat pipe failure scenario. For both heat pipe failure scenarios, the temperature increases around the failed heat pipe, and the boundary temperature for each heat pipe increases as close to the failed heat pipe. However, the fuel peak temperature does not increase significantly in the case of the peripheral heat pipe failure scenario, whereas the fuel peak temperature increases by 54 °C in the central heat pipe failure scenario.

In the case of structural analysis, each heat pipe failure scenario showed different results. For the peripheral heat pipe failure scenario, compared to the steady-state result, the thermal stress does not change greatly as shown in figure 4.26. This is because the temperature difference in the monolith was not increased as the failure of the outer heat pipe at initially low temperature was assumed. However, for the central heat pipe failure scenario, the thermal stress increases around the failed central heat pipe greatly as shown in figure 4.30. This is because the failed heat pipe is located where the temperature was initially high, the thermal

stress increased as the temperature difference within the monolith increased. These results indicate that the temperature distribution within the monolith has a significant influence on the stress. Especially, the temperature gradient within the monolith affects the stress greatly.



(a) Constant temperature boundary condition



(b) OpenFOAM-ANLHTP coupling

Figure 4.17 Minicore temperature calculation result in steady-state calculation

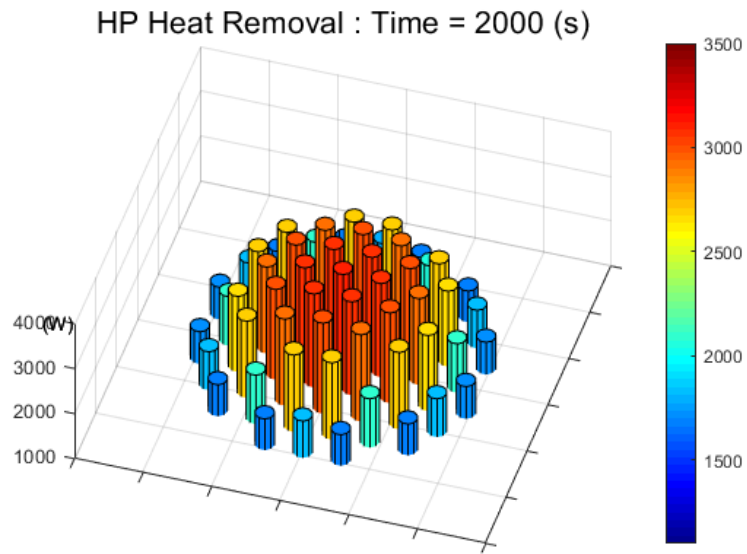


Figure 4.18 Heat removal rate of HPs in steady-state calculation

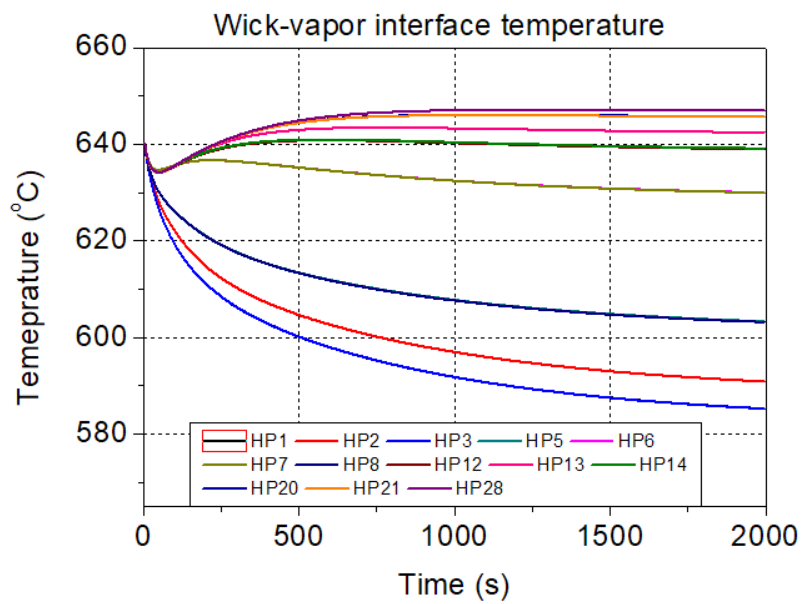


Figure 4.19 Boundary temperature of HPs in steady-state calculation

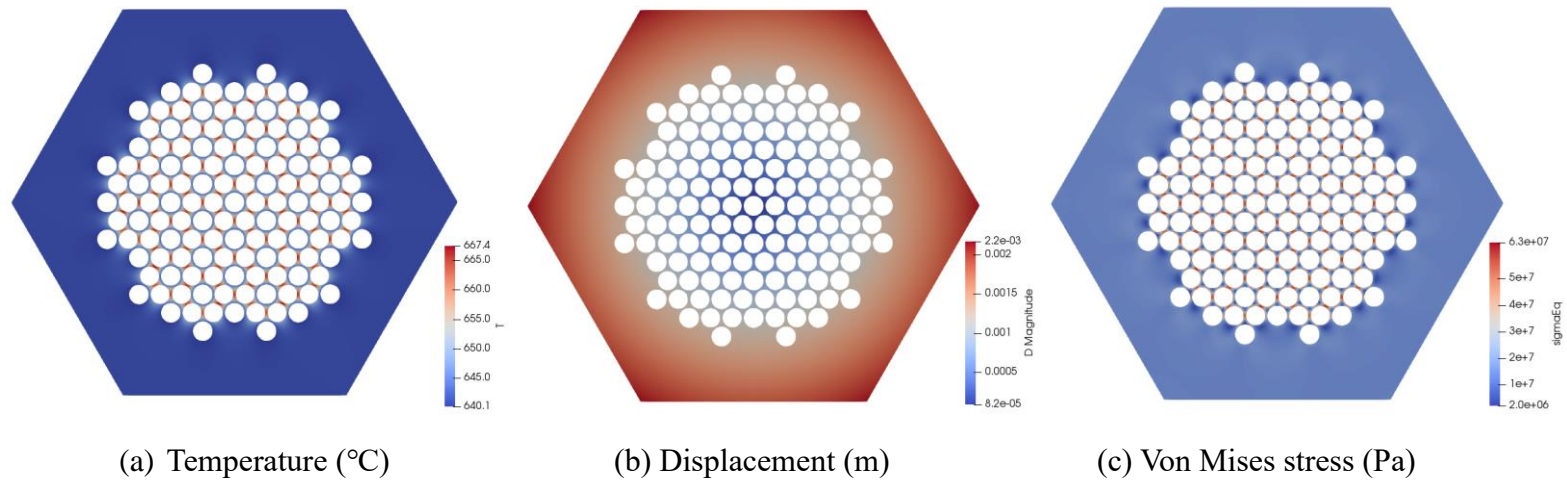


Figure 4.20 The stress analysis result of Minicore for constant temperature boundary case

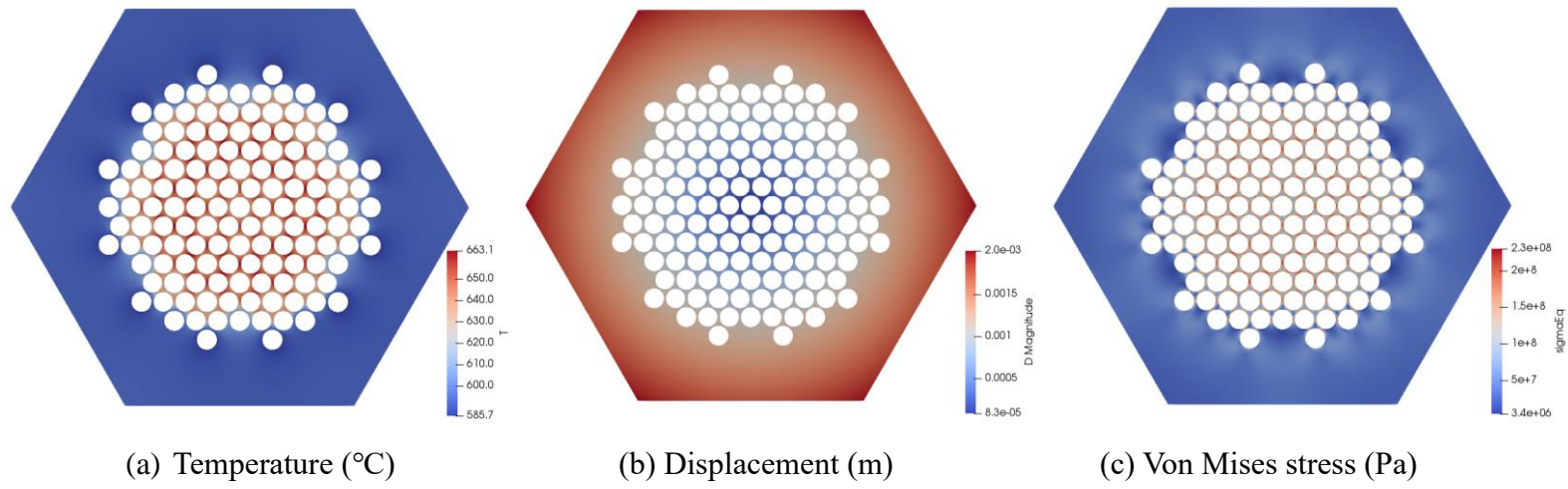


Figure 4.21 The stress analysis result of Minicore for OpenFOAM-ANLHTP coupling case

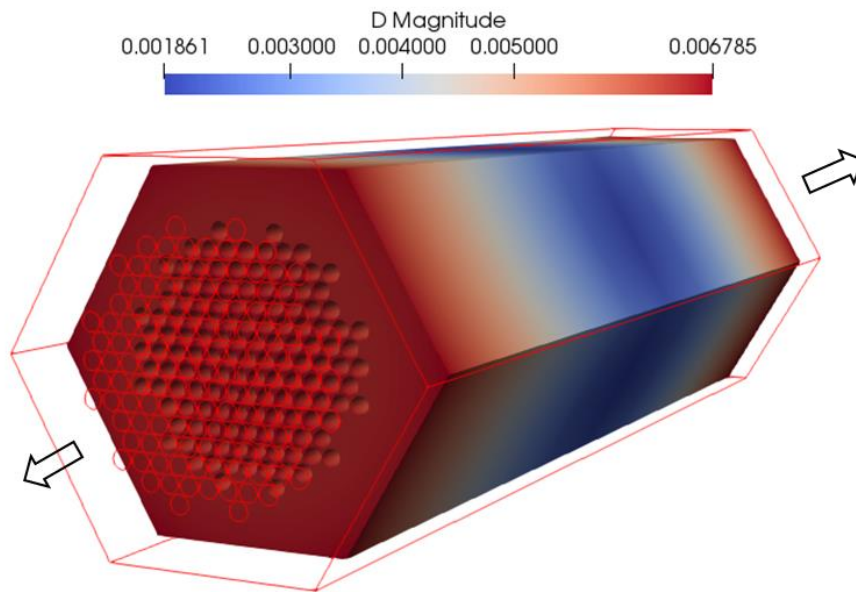


Figure 4.22 Volume expansion of unit cell in steady-state calculation (expanded volume was distorted for visibility)

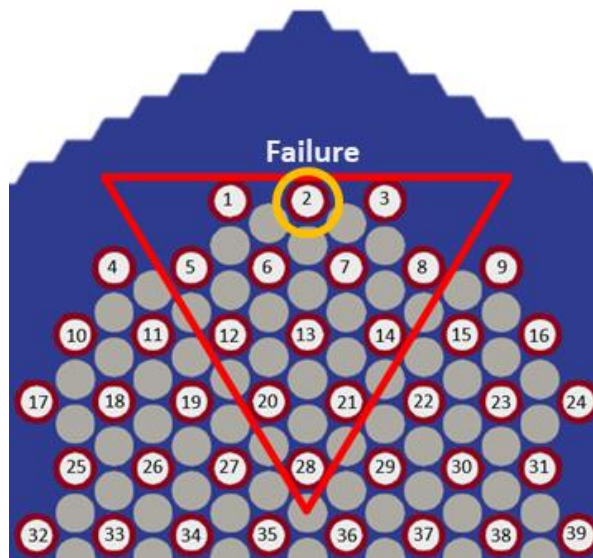


Figure 4.23 The peripheral heat pipe failure scenario

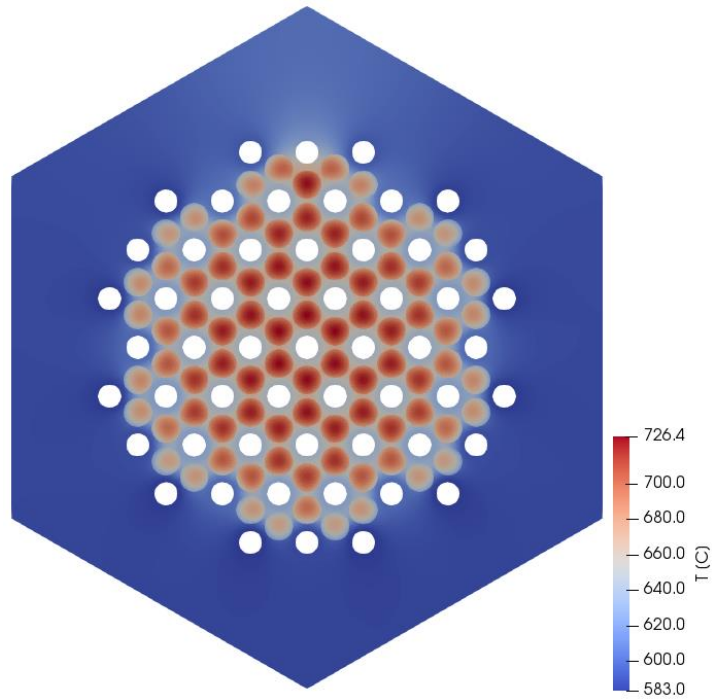


Figure 4.24 Temperature calculation results of the peripheral heat pipe failure scenario

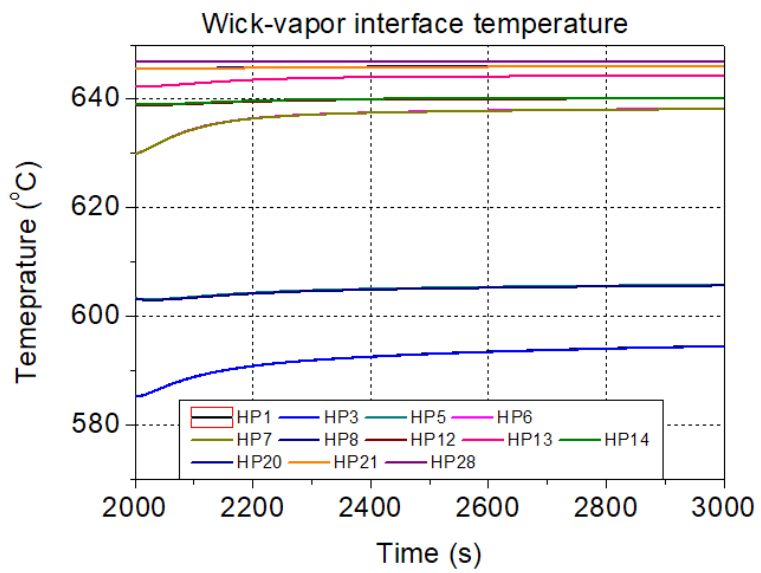


Figure 4.25 Wick-vapor interface temperature of the peripheral heat pipe failure scenario

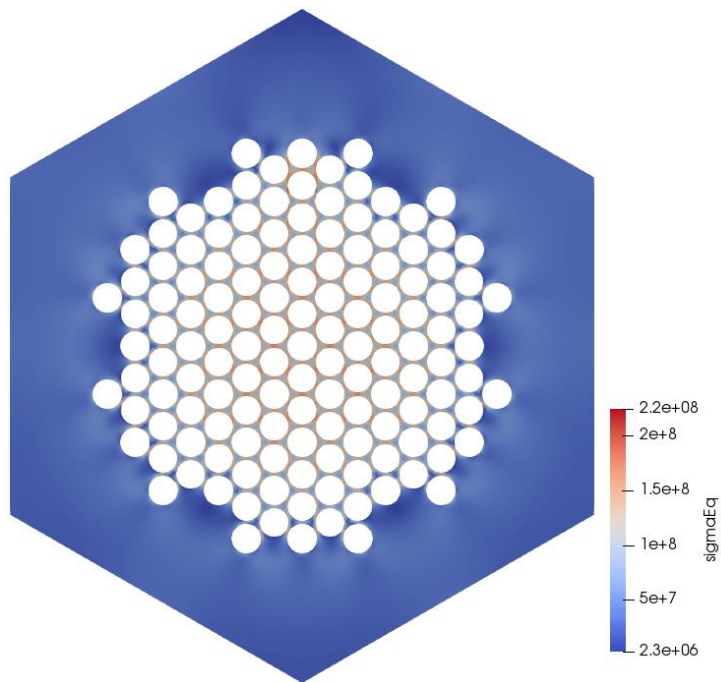


Figure 4.26 Stress calculation results of the peripheral heat pipe failure scenario

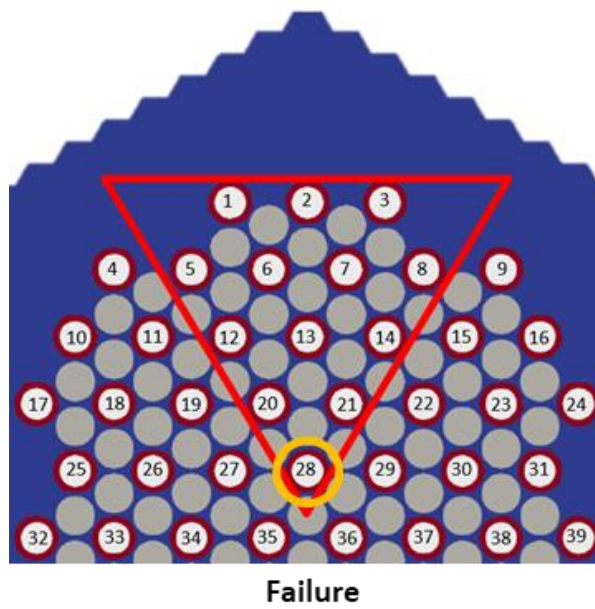


Figure 4.27 The central heat pipe failure scenario

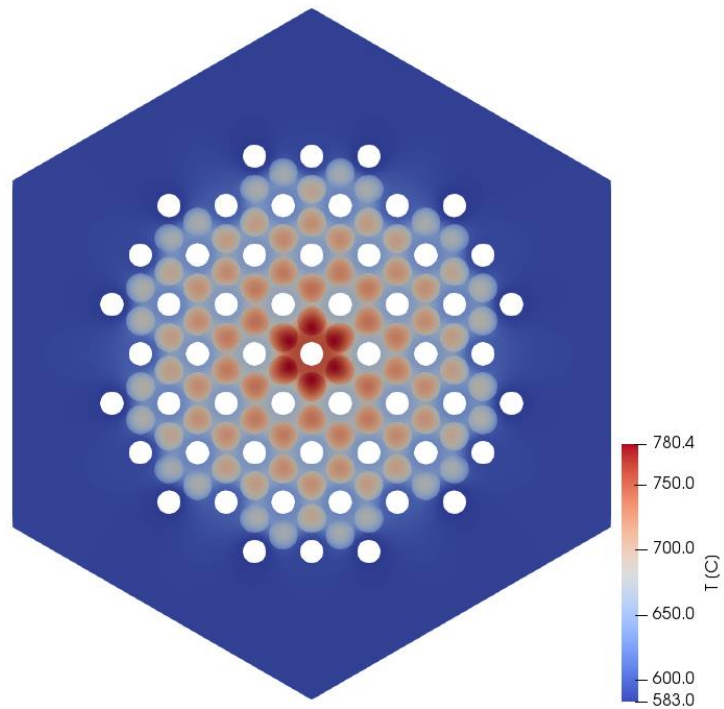


Figure 4.28 Temperature calculation results of the central heat pipe failure scenario

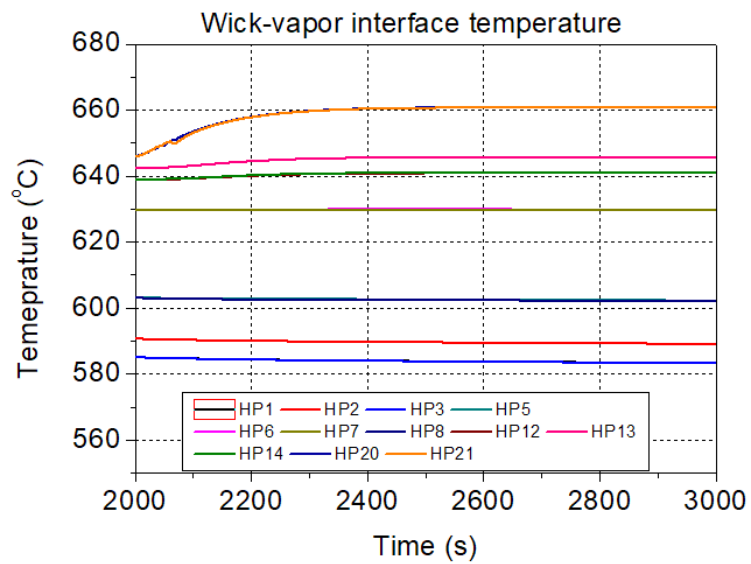


Figure 4.29 Wick-vapor interface temperature of the central heat pipe failure scenario

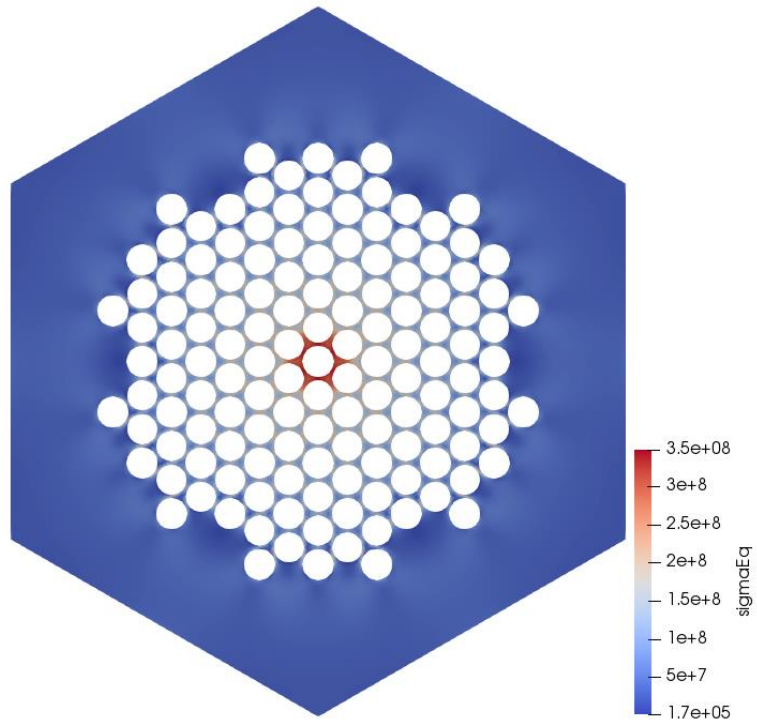


Figure 4.30 Stress calculation results of the central heat pipe failure scenario

4.2.3 Parametric study for design improvement

From the steady-state calculation and transient calculation of the Minicore, two aspects were confirmed: the current Minicore design does not satisfy the ASME maximum allowable stress limit, and the temperature distribution within the monolith has a great influence on the stress. Hence, to improve the Minicore design, the calculation was performed by adjusting the heat sink temperature of each heat pipe to flatten the temperature distribution in the monolith and make the stress lower. As shown in figure 4.31, the heat pipe was classified into 5 groups from inside to outside of the monolith, and in the coupling calculation, each group was calculated by ANLHTP with a different heat sink temperature. Meanwhile, if the heat sink temperature is too low, the heat pipe limit may not be satisfied as shown in figure 4.32, thus the heat sink temperature was increased to 451 °C. To flatten the temperature distribution of the monolith, the heat sink temperatures were adjusted to lower in high-temperature locations and higher in low-temperature locations. These adjusted heat sink temperature for each heat pipe group are shown in table 4.4. Using these heat sink temperature distribution, thermal analysis and stress analysis of Minicore were conducted.

Figures from 4.33 to 4.35 show the thermal analysis results of each heat sink temperature distribution case. As shown in figures, the fuel peak temperature decreases by about 20 °C by lowering the heat sink temperature of the central heat pipe group 1 and 2, and the temperature is flattened in case 2 and case 3 compared to case 1. In the same way as the previous calculations, the stress analysis was conducted using the temperature distribution from the thermal analysis results. Figure 4.36 and figure 4.37 show the temperature distribution of the monolith for each case and the stress analysis results for each case respectively. As shown in

the figure, the peak temperature at the center of the monolith is reduced and flattened in case 2 and case 3, and as the temperature distribution within the monolith flattened, the thermal stress also decreased. However, although the stress decreased greatly from 300 MPa of case 1 to 250 MPa of case 3, it still exceeds the ASME maximum allowable stress. Therefore, in addition to adjusting the heat sink temperature, it is necessary to further lower the stress through reducing power or geometric change.

Table 4.4 The heat pipe heat sink temperature of the Minicore problem

Group	1	2	3	4	5
Case 1	451	451	451	451	451
Case 2	401	401	451	451	451
Case 3	401	401	451	451	471

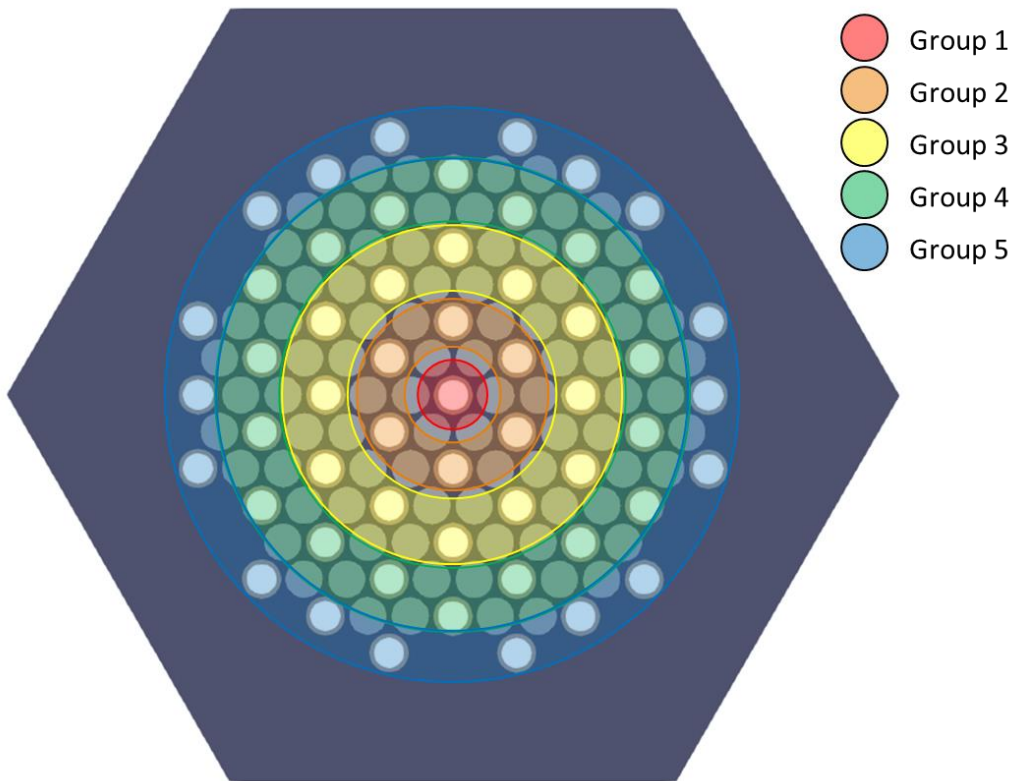


Figure 4.31 Heat pipe classification of the Minicore problem

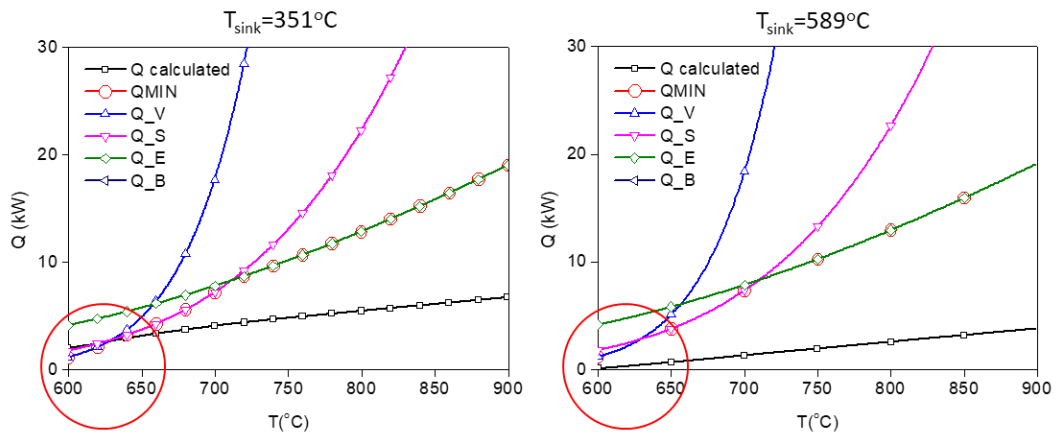


Figure 4.32 Heat pipe classification of the Minicore problem

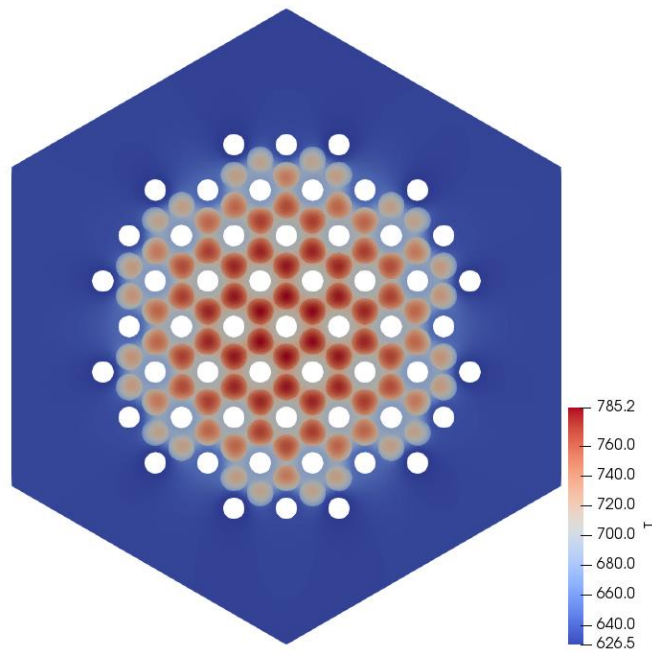


Figure 4.33 Temperature calculation results of the Minicore with the heat pipe sink temperature distribution case 1

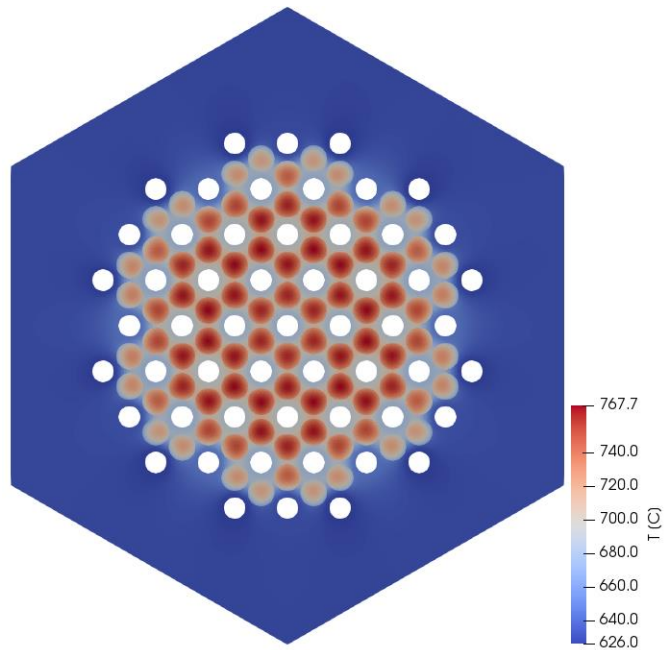


Figure 4.34 Temperature calculation results of the Minicore with the heat pipe
sink temperature distribution case 2

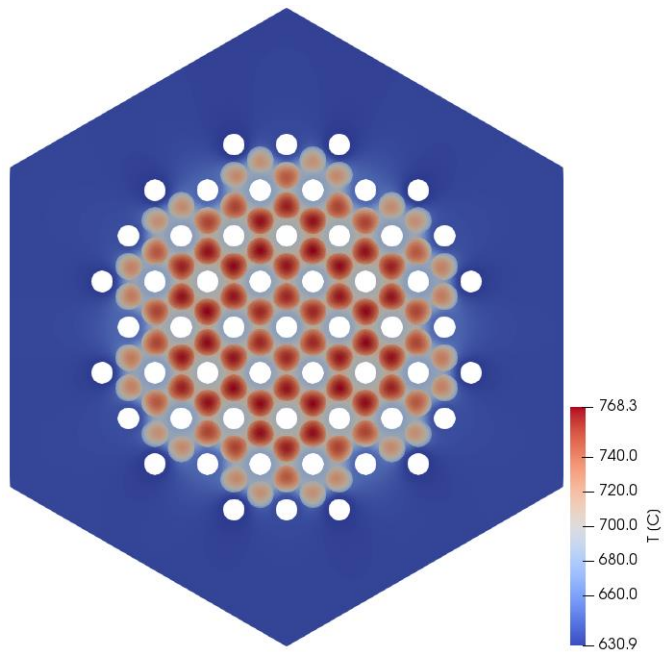
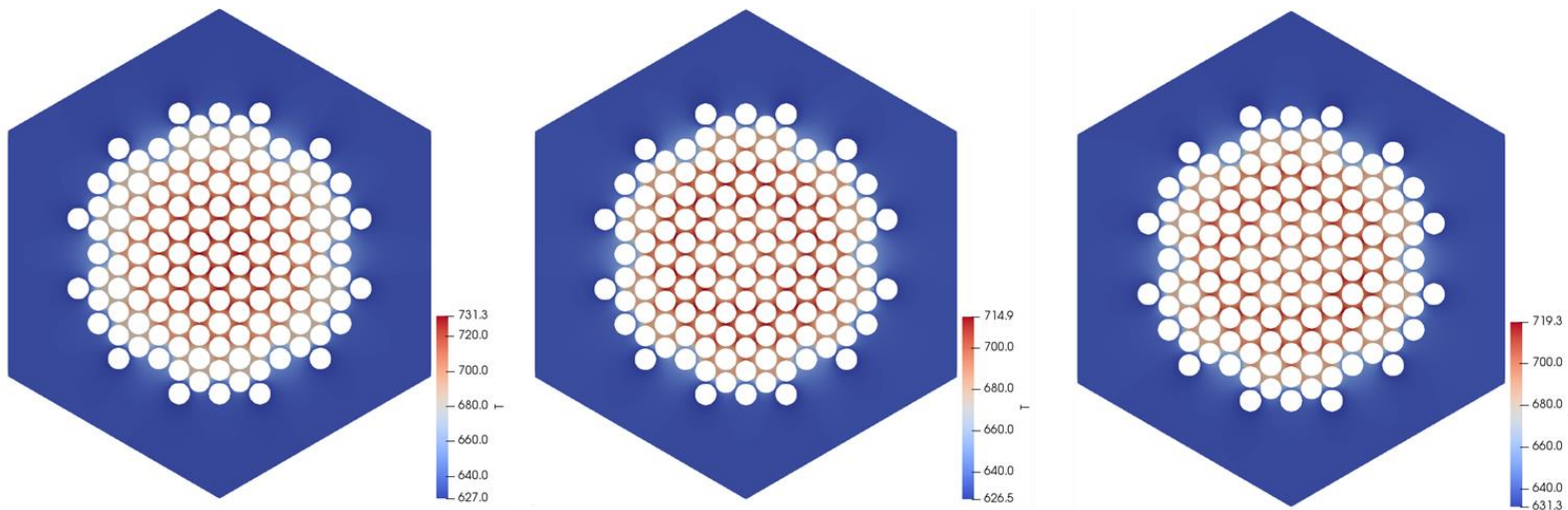


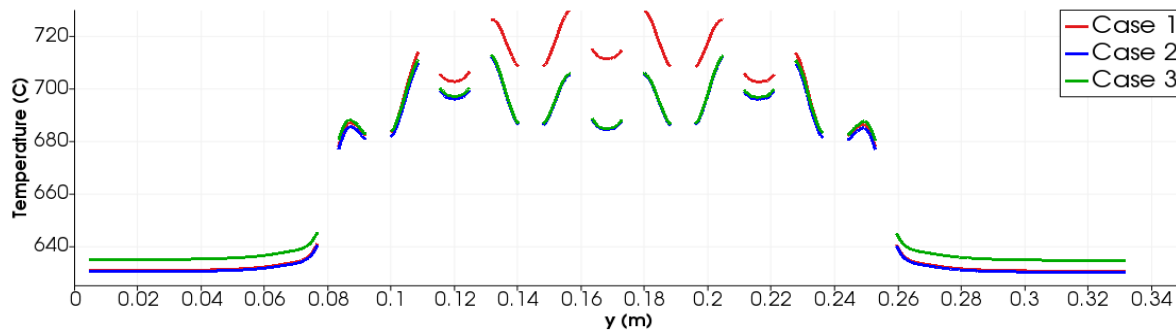
Figure 4.35 Temperature calculation results of the Minicore with the heat pipe
sink temperature distribution case 3



(a) Case 1

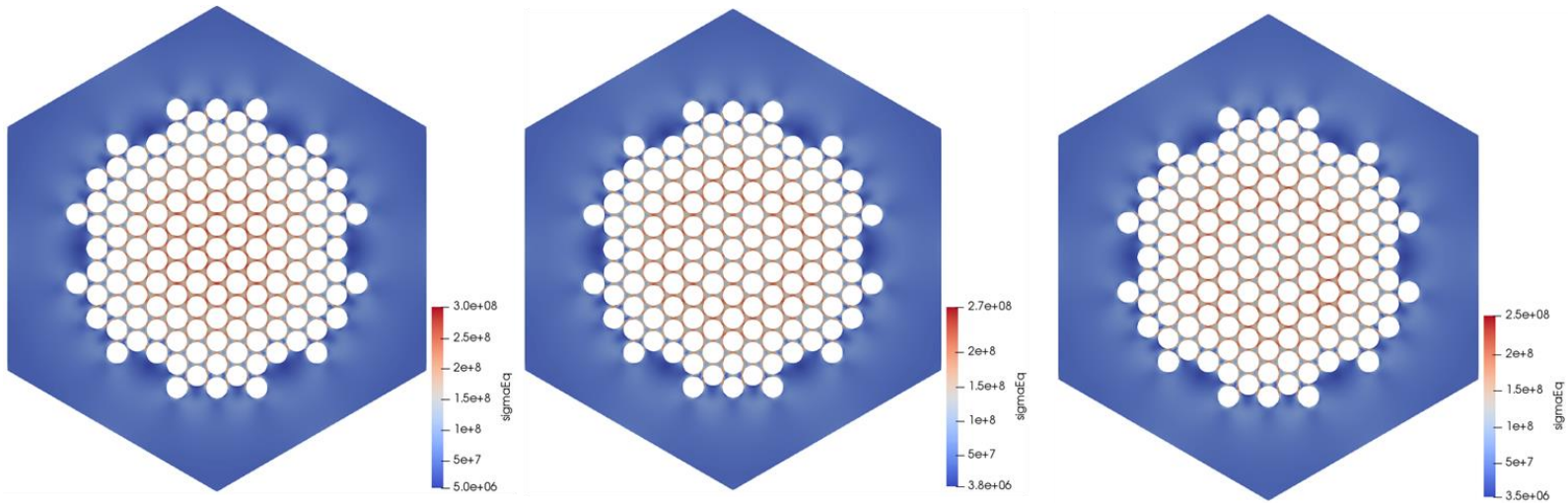
(b) Case 2

(c) Case 3



(d) Temperature distribution of 3 cases at $x=0.0075\text{m}$

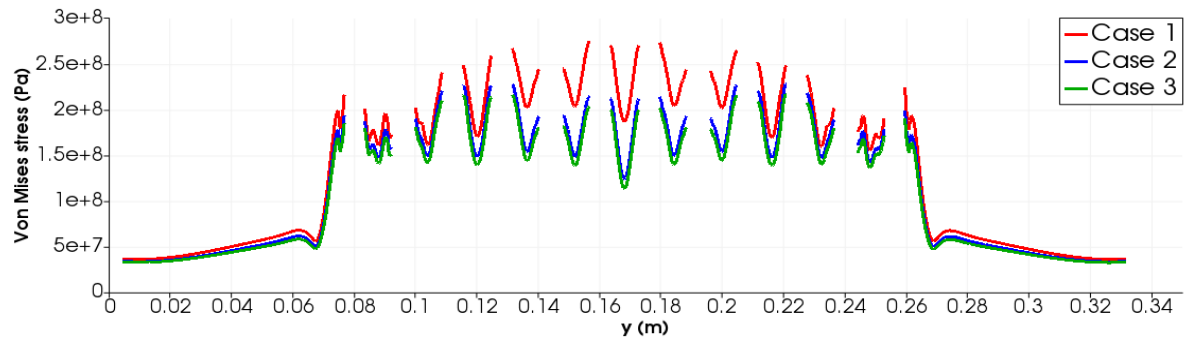
Figure 4.36 Temperature distributions of the monolith for different heat sink temperature



(b) Case 1

(b) Case 2

(c) Case 3



(d) Von Mises stress distribution of 3 cases at $x=0.0075\text{m}$

Figure 4.37 Stress analysis results for different heat sink temperature

Chapter 5. Conclusions

5.1 Summary

In the present study, the coupling of the thermal-structural analysis code OpenFOAM and the heat pipe thermal analysis code ANLHTP was performed as a framework to develop a high fidelity multi-physics simulation tool for the heat pipe cooled micro reactor. In this process, verification and improvement of the OpenFOAM solid mechanics solver, OpenFOAM-ANLHTP code coupling, and demonstration of the coupled code were performed.

First, the improvement of the OpenFOAM solid mechanics solver was conducted. Verification of the thermal-structural analysis solver was performed and the solver was modified for code coupling. After the modification, the solver is able to handle multiple materials and their varying properties with temperature. In addition, an external volumetric heat field was implemented for coupling with neutronics code in the future.

Next, a coupling system between OpenFOAM and ANLHTP was established. For the code coupling, a new boundary condition for external data exchange on a solid surface was added to OpenFOAM, and Python code was used to control the coupled code. To compensate for the limit of ANLHTP and reflect the axial temperature distribution, the location at which variables are exchanged between OpenFOAM-ANLHTP was set as the wick-vapor interface. For the convergence

of boundary temperature, Picard iteration was used with the fixed point method and secant method during the transient calculation.

Finally, a demonstration of thermal-structural analysis of heat pipe cooled reactor core was performed in the steady-state and transient conditions using the coupled code to confirm the appropriateness of the coupling. Unit cell problem and Minicore problem were analyzed, and the analysis results were compared with the thermal-structural analysis results of the MegaPower reactor core performed by INL. From the thermal analysis results of the unit cell problem, it was qualitatively confirmed that the OpenFOAM-ANLHTP code coupling was properly performed. In addition, the stress calculation result was comparable to the analysis result performed by INL was presented. However, thermal-structural analysis results of the Minicore showed high thermal stress so that the current Minicore design could not satisfy the ASME maximum allowable stress limit. Because the temperature distribution of the monolith had a significant influence on the thermal stress, adjusted heat pipe sink temperature was tested to flatten the temperature distribution within the monolith. However, although the maximum stress of the monolith decreased adjusting the heat pipe sink temperature, it still did not satisfy the ASME maximum allowable stress limit. Therefore, the Minicore design needs further improvement and the OpenFOAM-ANLHTP coupled code could be used for this purpose.

5.2 Recommendations

In the future, the coupled code system requires further improvement to be used as a high fidelity multi-physics simulation tool for a micro reactor. A series of validations against the experimental database is necessary. Currently, OpenFOAM and ANLHTP are validated against experimental data separately as there is no experimental data adequate for the validation of the coupled code. Especially, experimental studies for transient conditions are required to confirm the validity of the assumption imposed on ANLHTP, which assumes 1D quasi-steady-state for the vapor core of the heat pipe. Moreover, the OpenFOAM structural analysis solver needs to be improved. The present solver requires more computational cells to achieve mesh convergence compared with a commercial structural analysis code, ANSYS. A comprehensive code-to-code benchmark is desired.

In terms of the design of the Minicore problem, the current thermo-fluid conditions do not satisfy the allowable limitations of thermal stresses. Several approaches are available for satisfactory design; flattening of the temperature field in the core to minimize the thermal stress, thickening the webbing structure, and the change of working fluid of the heat pipe from sodium to potassium to give more flexibility in varying the heat rejection rate and avoid the operational limits, etc. The coupled code can be used effectively in optimizing the design of the core that satisfies the acceptance criteria with sufficient margins.

References

ANSYS, Inc., (2013). “ANSYS Mechanical APDL Verification Manual Release 15.0”

Aufiero, M., Fiorina, C., Laureau, A., et al., (2015). “Serpent-OpenFOAM Coupling in Transient Mode: Simulation of A Godiva Prompt Critical Burst”, ANS MC2015, 2015

Autodesk, Inc. (2015). “Autodesk Nastran 2016 Verification Manual”

Chi, S. W., (1976). “Heat Pipe Theory and Practice: A Sourcebook”, McGraw Hill Book Company, New York

Choi, S. H., Jo, C. K., Lee, S. N., (2019). “Conceptual Core Design and Preliminary Neutronics Analysis for a Space Heat Pipe Reactor, Transactions of the Korean Nuclear Society Autumn Meeting

Dunn, P. and Reay, D. A., (1978). “Heat Pipes”, Pergamon Press, Oxford

Fiorina, C., Clifford, I., Aufiero, M., et al., (2015). “GeN-Foam: A Novel OpenFOAM Based Multi-physics Solver For 2D/3D Transient Analysis of Nuclear Reactors”, Nuclear Engineering and Design, Volume 294, pp. 24-37

Gibson, M. A., Poston, D. I., McClure, P., et al., (2018). “Kilopower Reactor Using Stirling Technology (KRUSTY) Nuclear Ground Test Results and Lessons Learned”, NASA/TM-2018-219941

Hu, G., Hu, R., Kelly, J. M., et al., (2019). “Multi-Physics Simulations of Heat Pipe Micro Reactor”, ANL-NSE-19/25

Kelly, C. T. (1995). Iterative Methods for Linear and Nonlinear Equations, Vol. 16 of Frontiers in Applied Mathematics, Philadelphia, PA: Society for Industrial and Applied Mathematics.

Lee, C. H., Jung, Y. S., Cho, H. K., (2019). “Micro Reactor Simulation Using the PROTEUS Suite in FY19”, ANL/NSE-19/33

Lee, K. M., Ohn, M. Y., Lim, H. S., et al., (1995). “Study on Models for Gap Conductance Between Fuel and Sheath for CANDU Reactors”, Ann. Nucl. Energy Vol. 22, No. 9, pp. 601-610

Los Alamos National Lab, (2018, September 20). “A Small Reactor to Bring Power to Remote Locations”, [Video file], Retrieved from https://www.youtube.com/watch?v=RPI8G6COc8g&feature=emb_title

Martineau, R. C., (2019). “DireWolf: MOOSE-based Multiphysics Simulator for Megawatt Scale Micro-Reactor”, GAIN-EPRI-NEI-IS NIC Mirco-Reactor Workshop

McClure, P. R., Dixon, D. D., Poston, D. I., et al., (2020). United States Patent Application Publication, US 2020/0373029 A1

OKLO, (2020). “Part II: Final Safety Analysis Report”

Rampal, B., (2020). “CATF Welcomes the First Non-Light Water Reactor License Application to the Nuclear Regulatory Commission”, Clean Air Task Force, Retrieved from <https://www.catf.us/2020/03/catf-welcomes-first-non-light-water-reactor-license-application/>

Sterbentz, J. W., Werner, J. E., McKellar, M. G., et al., (2017). “Special Purpose Nuclear Reactor (5MW) for Reliable Power at Remote Sites Assessment Report Using Phenomena Identification and Ranking Tables (PIRTs)”, INL/EXT-16-40741

Sterbentz, J. W., Werner, J. E., Hummel, A., J., et al., (2018). “Preliminary Assessment of Two Alternative Core Design Concepts for the Special Purpose Reactor”, INL/EXT-17-43212

Tak, N., I., Lee, S., N., (2020). “Transient Lumped Parameter Analysis of Heat Pipe for a Space Nuclear Reactor”, Transactions of the Korean Nuclear Society Virtual Spring Meeting

The OpenFOAM Foundation, “OpenFOAM v7 User Guide”, accessed Feb 01,
<https://cfd.direct/openfoam/user-guide-v7>

WestinghouseNuclear, (2019, September 17). “eVinci™ Micro Reactor” [Video
file], Retrieved from
https://www.youtube.com/watch?v=Sh6BKKFxN_g&feature=emb_title

Zuo, Z. J., Faghri, A., (1998). “A Network Thermodynamic Analysis of the Heat
Pipe,” Int. J. Heat Mass Transfer, Volume 41, Issue 11, pp. 1473-1484

국문초록

최근 다양한 형태의 초소형 원전 설계가 제시되고 그에 대한 연구가 진행되고 있으며, 그 중 히트파이프 냉각 원자로가 주목받고 있다. 히트파이프 원자로는 모놀리스라는 고체 구조물에 다수의 연료봉과 히트파이프가 설치된 형태의 노심을 갖고 있다. 히트파이프 냉각 원자로는 작은 디자인과 설치가 쉬운 휴대성, 향상된 계통 신뢰도와 안정성이라는 장점이 있다. 히트파이프 냉각 원자로의 개발은 미국의 LANL, 웨스팅하우스와 OKLO에 의해 주도되고 있다.

이러한 히트파이프 냉각 원자로의 노심설계에는 고려해야할 몇 가지 이슈가 있다. 육상용 히트파이프 원자로는 수 MW의 출력을 위해 연료봉과 히트파이프의 집적이 필요하다. 이러한 집적은 구조 내 온도 구배를 상승시키고 높은 열응력을 발생시켜 구조건전성을 저하시킨다. 또한 높은 온도와 잦은 부하추종으로 인한 출력변동에 의해 고체 노심의 체적팽창이 발생하고 중성자 누출이 변하면서 반응도 궤환이 발생한다. 또한 실제 히트파이프 냉각 원자로 운전 시의 안전 기준이 존재하며, 이는 각 원자로 특성마다 다르게 나타나므로 정확한 해석이 중요하다.

히트파이프 원자로 노심의 정확한 해석을 위해서는 높은 정확도의 다물리 해석이 필요하며, 이를 위해 히트파이프 열해석 코드와 노심 열구조해석 코드의 연계계산이 필요하다. 이를 위해 INL, KAERI에서 히트파이프 원자로 노심 해석에 대한 연구를 수행하였으며, 서울대학교 역시 ANL과 협력하여 히트파이프 원자로 노심 연계계산 연구를 수행한

바 있다.

본 연구의 목적은 높은 정확도의 다물리해석 툴을 개발하여 히트파이프 냉각 원자로의 디자인 신뢰성과 안전해석을 개선하는 것이다. 이를 위해 다물리 해석에 필요한 기본적인 스트레스 및 팽창 계산이 가능한 솔버를 제공하며, 오픈소스 기반으로 솔버 개선이 용이한 OpenFOAM을 사용하였다.

히트파이프 냉각 원자로 노심의 열응력 해석을 위해 OpenFOAM 솔버를 개선하였다. 기존 `solidDisplacementFoam` 솔버를 수정하여 복합조성에 대해 계산할 수 있도록 하였으며, 온도에 따른 물성치 변화를 반영할 수 있도록 하였다. 또한 중성자 코드와의 연계를 위한 외부 체적열 정보를 읽어들이 수 있도록 하였으며, 고체 경계에서의 연계를 위한 외부 데이터 교환 경계조건을 추가하였다.

OpenFOAM과 히트파이프 코드인 ANLHTP의 연계 체계를 구축하였다. OpenFOAM과 ANLHTP는 파이썬 코드를 통해 외부적으로 연계 되었으며, OpenFOAM은 경계에서의 열교환량을 제공하고 ANLHTP는 벽면 온도를 전달했다. ANLHTP의 단점을 보완하고 축방향 온도분포를 반영할 수 있도록 변수가 교환되는 위치는 히트파이프 내부의 워 구조와 기체 경계면으로 설정되었다. 이 때 경계 온도를 수렴시키기 위하여 `fixed point` 방법과 `secant` 방법을 이용하여 `Picard iteration`을 수행하였다.

연계의 적절성을 확인하고자 OpenFOAM-ANLHTP 연계 코드를 이용하여 정상상태 및 과도상태에서 노심 열-구조해석을 수행하였다. 각각 단위 격자(7HP) 문제와 미니코어 문제를 해석하였으며, 연계 계산 결과

모놀리스와 연료봉의 온도 분포 및 모놀리스에서의 열응력 분포를 확인할 수 있었다. INL에서 수행한 MegaPower 원자로 노심 해석 결과와 온도 및 최대 응력 비교를 진행하여 연계 코드가 잘 작동함을 정성적으로 확인하였다.

주요어: 다물리 해석, 초소형 원자로, 원자로 노심 해석, 열-구조 해석, 응력 해석, OpenFOAM, 히트파이프,

학번: 2019-20171

감사의 글

2년동안 너무나도 부족한 것이 많았음에도 많은 분들의 도움을 받아 무사히 졸업할 수 있게 되었습니다.

먼저 지도해주신 조형규 교수님께 감사드립니다. 처음 입학할 때부터 안좋은 모습을 많이 보여드렸음에도 불구하고 저를 올바른 방향으로 이끌어주신 덕분에 수많은 시행착오를 겪으면서도 여기까지 올 수 있었습니다. 박사과정에 진학해서도 교수님의 지도를 통해 더욱 성장하도록 하겠습니다.

그리고 지식 뿐 아니라 삶에 대한 가르침을 아끼지 않아주신 박군철 선생님 감사합니다. 연구자로서 항상 정진하면서 선생님의 가르침을 잊지 않도록 하겠습니다.

바쁘신 중에도 시간 내어주시고 심사 맡아주신 김응수 교수님 감사합니다. 수업을 들을 때, 심사를 받을 때, 박사과정 면접을 볼 때에도 교수님의 친절함을 통해 마음을 편하게 가질 수 있었습니다. 그리고 마찬가지로 심사 맡아주신 원자력연구원의 박병하 박사님 감사합니다. 연구 내용 관련하여 조언해주신 내용 덕분에 많은 점을 배울 수 있었고 연구를 더욱 개선하여 이렇게 무사히 졸업할 수 있게 된 것 같습니다.

그리고 2년동안 많은 도움을 주고 추억을 선사해준 연구실 구성원들에게도 감사드립니다. 지금은 졸업해서 다른 곳에서 각자의 일에 충실할 재순이 형, 희수 누나, 재호 형, 유연이 누나 모두 감사했습니다. 연구실 맏형으로서 항상 중심을 잡아주시는 치진이 형, 현 랩장이자 모든

것이 뛰어난 건우 형, 같은 자리에서 항상 수많은 도움을 주시는 205호 대장 신엽이 형, 원안위 때부터 많은 걸 알려주신 창원이 형, 같은 주제로 연구를 진행하면서 연구에 가장 큰 도움을 준 산이 형, 연구실 선배이자 가장 든든한 친구인 진성이, 군 위탁생 역사에 한 획을 그으신 상욱이 형, 곧 더 멋진 모습으로 돌아올 장근이 형, 후배지만 저보다 더 뛰어난 모습을 보여주는 형주, 그리고 앞으로 오랜 시간을 함께 보내게 될 희표까지 모두 감사합니다.

앞으로 연구를 같이 진행하게 될 주한규 교수님 연구실의 재욱이와 경민이, 그리고 한규형에게도 감사를 전합니다. 대학원에 들어오기 전에도 많은 도움을 받았었고 앞으로도 더 많은 도움을 받게 될 것 같아 미리 감사를 전합니다.

그리고 고등학교 때부터 공부밖에 할 줄 모르던 저를 응원해준 친구들에게 고맙다고 전하고 싶습니다. 특히 다른곳에서 이미 대학원 생활을 하고 있거나 앞으로 대학원 생활을 하게 될 그 친구들을 응원합니다.

마지막으로 언제나 내 인생의 버팀목이 되어주고 앞으로도 내 인생의 모든 것을 차지할 우리 가족 고맙습니다. 공부만 하고있는 아들 뒷바라지 하느라 고생하시는 부모님과 동생 챙겨주는 형, 모두 감정 표현에 인색하여 말로 잘 전하지는 못했었지만 항상 사랑하고 박사 과정 동안에도 우리 가족 모두 화목하고 행복했으면 합니다.

2년 간의 석사과정을 마치고 이제는 박사과정 정명진으로 돌아오겠습니다. 모두들 감사합니다.